Quaternary Science Reviews 189 (2018) 149–168

Contents lists available at ScienceDirect

Quaternary Science Reviews

journal homepage: www.elsevier.com/locate/quascirev

Glacially induced faulting along the NW segment of the Sorgenfrei-Tornquist Zone, northern Denmark: Implications for neotectonics and Lateglacial fault-bound basin formation

Christian Brandes [a, *], Holger Steffen [b], Peter B.E. Sandersen [c], Patrick Wu [d], Jutta Winsemann [a]

[a] Institut für Geologie, Leibniz Universität Hannover, Callinstr. 30, 30167, Hannover, Germany
[b] Lantmäteriet, Geodetic Infrastructure, Lantmäterivägen 2C, 80102, Gävle, Sweden
[c] GEUS - Geological Survey of Denmark and Greenland, Department of Groundwater and Quaternary Geology Mapping, C. F. Møllers Allé 8, Building 1110, 8000, Århus C, Denmark
[d] Department of Earth Sciences, The University of Hong Kong, Pokfulam Road, Hong Kong

ARTICLE INFO

Article history:
Received 15 November 2017
Received in revised form
23 March 2018
Accepted 28 March 2018
Available online 24 April 2018

Keywords:
Sorgenfrei-Tornquist Zone
Neotectonics
Glacially induced faulting
Børglum fault
Finite element modelling
Coulomb failure stress
Soft-sediment deformation structures

ABSTRACT

The Sorgenfrei-Tornquist Zone (STZ) is the northwestern segment of the Tornquist Zone and extends from Bornholm across the Baltic Sea and northern Denmark into the North Sea. It represents a major lithospheric structure with a significant increase in lithosphere thickness from south to north. A series of meter-scale normal faults and soft-sediment deformation structures (SSDS) are developed in Lateglacial marine and lacustrine sediments, which are exposed along the Lønstrup Klint cliff at the North Sea coast of northern Denmark. These deformed deposits occur in the local Nørre Lyngby basin that forms part of the STZ.

Most of the SSDS are postdepositional, implying major tectonic activity between the Allerød and Younger Dryas (~14 ka to 12 ka). The occurrence of some syn- and metadepositional SSDS point to an onset of tectonic activity at around 14.5 ka. The formation of normal faults is probably the effect of neotectonic movements along the Børglum fault, which represents the northern boundary fault of the STZ in the study area.

The narrow and elongated Nørre Lyngby basin can be interpreted as a strike-slip basin that developed due to right-lateral movements at the Børglum fault. As indicated by the SSDS, these movements were most likely accompanied by earthquake(s). Based on the association of SSDS these earthquake(s) had magnitudes of at least $M_S \geq 4.2$ or even up to magnitude ~ 7 as indicated by a fault with 3 m displacement. The outcrop data are supported by a topographic analysis of the terrain that points to a strong impact from the fault activity on the topography, characterized by a highly regular erosional pattern, the evolution of fault-parallel sag ponds and a potential fault scarp with a height of 1–2 m.

With finite-element simulations, we test the impact of Late Pleistocene (Weichselian) glaciation-induced Coulomb stress change on the reactivation potential of the Børglum fault. The numerical simulations of deglaciation-related lithospheric stress build-up additionally support that this neotectonic activity occurred between ~14.5 and 12 ka and was controlled by stress changes that were induced by the decay of the Scandinavian ice sheet. In the Holocene, the stress field in the study area thus changed from GIA-controlled to a stress field that is determined by plate tectonic forces.

Comparable observations were described from the central STZ in the Kattegat area and the south-eastern end of the STZ near Bornholm. We therefore interpret the entire STZ as a structure where glacially induced faulting very likely occurred in Lateglacial times. The fault reactivation was associated with the formation of small fault-bound basins that provided accommodation space for Lateglacial to Holocene marine and freshwater sediments.

* Corresponding author.
E-mail address: brandes@geowi.uni-hannover.de (C. Brandes).

https://doi.org/10.1016/j.quascirev.2018.03.036

1. Introduction

The decay of the Late Weichselian (MIS 2) Scandinavian ice sheet has induced large stress changes in the lithosphere that led to reactivation of pre-existing faults. Such glacially reactivated faults were named glacially induced, end-glacial or post-glacial faults (Lund, 2015), and we use the term *glacially induced fault* in the following. The activity along these faults was accompanied by earthquakes that reached large magnitudes. Paleoseismological studies show that magnitudes >6 M_w occurred at ~13–9 ka along glacially induced faults in Scandinavia (Arvidsson, 1996; Mörner, 2011) and the areas, where glacially induced faulting took place are still the most seismically active areas in Fennoscandia (Arvidsson, 1996; Ojala et al., 2004; Lindblom et al., 2015).

Glacially induced faults are well known and have been investigated in northern Fennoscandia for more than 40 years. First evidences were found in the 1960s and 1970s (e.g., Kujansuu, 1964; Lagerbäck, 1978; Mörner, 1978). Over the years, several glacially induced faults were identified, mainly in northern Norway, Sweden and Finland (Arvidsson, 1996; Dehls et al., 2000; Gregersen, 2002; Lagerbäck and Sundh, 2008; Kukkonen et al., 2010; Sutinen et al., 2014; Mikko et al., 2015; Palmu et al., 2015; Ojala et al., 2017). In recent times, more glacially induced faults were suggested for the central and southern part of Scandinavia (Jensen et al., 2002; Smith et al., 2014; Jakobsson et al., 2014; Berglund and Dahlström, 2015; Malehmir et al., 2016; Al Hseinat and Hübscher, 2014, 2017). All these faults have in common that they were covered by the Scandinavian ice sheet during the Late Weichselian. However, studies of Brandes et al. (2012), Brandes and Tanner (2012), Brandes and Winsemann (2013), Brandes et al. (2015) and Sandersen and Jørgensen (2015) imply that glacially induced faults were also developed outside the former glaciated area, in southern Denmark and northern Germany. Glacially induced faulting is also suggested for northeastern Germany, Poland and the Baltic countries (Hoffmann and Reicherter, 2012; van Loon & Pisarska-Jamroży, 2014; van Loon et al., 2016). These findings generally support the conceptual model of stress relief phenomena due to glaciation in Stewart et al. (2000) as well as finite element modelling results of the glaciation-solid Earth interaction (Wu and Hasegawa, 1996a; Hampel et al., 2009; Steffen et al., 2014b; Brandes et al., 2015).

In view of the regional distribution of discovered or suggested glacially induced faults there appears to be a gap of field evidences in northern Denmark. However, numerical simulations also here support a likely reactivation potential for preexisting faults in the area (see supplementary information in Brandes et al., 2015), which suggests a careful geological re-analysis of northern Denmark regarding glacially induced faults. We therefore turn to the Børglum fault in northern Denmark (Fig. 1), which forms part of the Sorgenfrei-Tornquist Zone (STZ). Kristensen et al. (2013) identified fault motion in postglacial sediments of this area and suggested glacial rebound, among others, as a possible driving force.

We present new insights into the neotectonic activity of the Børglum fault and thus the STZ by combining newly gained field data from the Lønstrup Klint section, analysis of high-resolution LiDAR terrain data and numerical simulations based on a new generation of high-resolution (in time and space) finite element models that test lateral variations in the subsurface and two different ice history models. We show that young seismic activity in this area was triggered by the decay of the Late Pleistocene (MIS 2) Scandinavian ice sheet. We argue that the STZ is susceptible to glacially induced faulting. Understanding the formation and distribution of glacially induced faults is of great societal relevance and analysing the controlling factors of this type of seismicity is an important step towards a profound hazard risk evaluation for e.g. major infrastructure construction such as new nuclear power plants or underground transport, and ground stability in view of potential liquefaction or landslide processes. We further show that the fault reactivation in the study area was associated with the formation of small fault-bound basins that provided accommodation space for Lateglacial to Holocene marine and lacustrine sediments. These mini-basins partly contain important Late Paleolithic artifacts, which record some of the northernmost traces of human presence in Northwestern Europe during the Lateglacial (Fischer et al., 2013).

2. Geological setting

2.1. The Sorgenfrei-Tornquist Zone

The Tornquist Zone is a major lithospheric structure that extends from the Central North Sea across Denmark and the Baltic Sea into Poland (Fig. 1). It is subdivided into a northwestern segment referred to as the Sorgenfrei-Tornquist Zone (STZ) and a southeastern part referred to as the Teisseyre-Tornquist Zone (TTZ) (Pedersen et al. 1999; Erlström et al., 1997; Phillips et al., 2017) (Fig. 1). Although questioned by some authors (e.g., Berthelsen, 1998), the TTZ has traditionally been interpreted as the southern limit of Baltica consequently marking the boundary between Baltica and the Avalonia terrane. Avalonia is a terrane that was accreted to the continent Baltica during the Caledonian orogeny (Tanner and Meissner, 1996). Between Baltica and Avalonia the so-called Tornquist Sea was subducted in Ordovician to Silurian times (Torsvik and Rehnström, 2003). Based on data from Poland, Mazur et al. (2015) placed the southern margin of Baltica further to the south and interpreted the Tornquist Line in that area as an intraplate feature. This new result started a discussion about the nature of the TTZ (Mazur et al., 2015, 2016; Narkiewicz and Petecki, 2016). New data from Smit et al. (2016) also shift the southern margin of Baltica further southward towards the Elbe Lineament. The Elbe Lineament is a crustal boundary in northern Germany (Bayer et al., 1999) that is marked by a drop in P-wave velocity (e.g. Scheck et al., 2002). In previous studies this lineament was interpreted as an intra-Avalonian structure (Krawczyk et al., 2008) or as a strike-slip fault that defines the northeastern extent of the eastern Avalonia terrane and the southwestern margin of the Fennoscandian shield (Tanner and Meissner, 1996).

The STZ in northern Denmark is interpreted as a major tectonic structure that separates the Danish Basin from the Fennoscandian Shield (Hansen et al., 2000) and is considered to be a deep-seated fault zone between two crustal blocks (Mogensen, 1994; Mogensen and Korstgård, 2003). The STZ is bounded by the Grenå-Helsingborg fault in the south and by the Børglum fault in the north (Mogensen, 1994; Mogensen and Korstgård, 2003) (Figs. 1 and 2A). In the study area the Fjerritslev fault, as a prolongation of the Grenå-Helsingborg fault, forms the southern margin of the STZ. Along the Børglum fault, 7 km of right lateral displacement was estimated from the Late Paleozoic to the present-day (Mogensen, 1994). The development of the STZ was probably controlled by weakening of the Baltic (Fennoscandian) Shield due to the Caledonian deformation (Thybo, 1997). In the Late Carboniferous to the Early Permian, the area underwent rifting (Michelsen, 1997), caused by a widening of the TTZ into northern Denmark (Thybo, 1997, 2000). The STZ was reactivated in Triassic to Jurassic times under an extensional stress regime (Hansen et al., 2000). During the Late Cretaceous to Early Paleogene the STZ underwent contraction and inversion (Michelsen and Nielsen, 1993; Huuse et al., 2001; Kley and Voigt, 2008). Two inversion phases are documented here: the first one took place during the Campanian and Maastrichtian, and a second inversion phase occurred in the late Danian (Nielsen et al., 2014). It seems that within the STZ, the

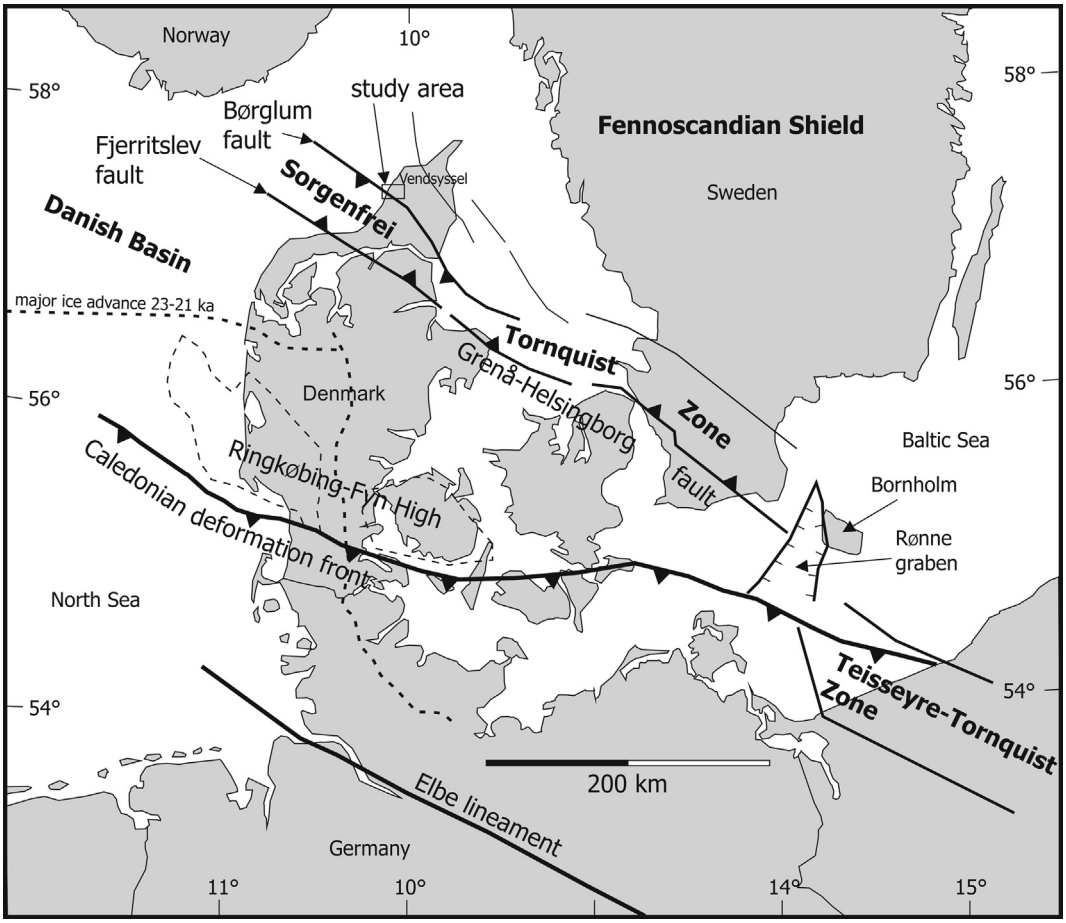

Fig. 1. Tectonic setting of the study area. The Sorgenfrei-Tornquist Zone extends between the North Sea in the north and Bornholm in the south. The black rectangle indicates the study area. Map is based on Thybo (1997). The limit of the ice advance at 23–21 ka is based on Larsen et al. (2009).

Børglum fault was the most active fault during the inversion (Hansen et al., 2000). The estimated uplift for the STZ during the Late Mesozoic - Early Cenozoic inversion phase is in a range of 1700–2000 m (Michelsen and Nielsen, 1993). Rasmussen (2009) showed that there was also Neogene inversion in the North Sea area. Late Mesozoic to Cenozoic inversion and uplift also affected parts of northern Germany (e.g., Kley and Voigt, 2008; Brandes et al., 2013) and the British Isles (e.g., Williams et al., 2005; Holford et al., 2005, 2009; Hillis et al., 2008). Today the area between the Børglum fault and the Grenå-Helsingborg fault is characterized by several small Mesozoic faults (Mogensen and Korstgård, 2003).

The STZ corresponds with a sharp increase in (seismically determined) lithosphere thickness (Cotte et al., 2002). South of the STZ, the lithosphere-asthenosphere boundary is at a depth of 120 ± 20 km, whereas in the north, the lithosphere-asthenosphere boundary is probably deeper than 200 km (Cotte et al., 2002). However, the earthquake activity in that area since 1930 forms a diffuse pattern that does not indicate a sharp delineation of tectonic units (Gregersen et al., 2005).

The faults of the STZ have been intermittently active from the Precambrian until recent times (Mogensen and Korstgård, 2003) but Denmark, including the STZ, is presently characterized by low seismic activity (Gregersen and Voss, 2009). In recent years the Danish area has experienced minor earthquakes, but according to Gregersen and Voss (2012, 2014) even the STZ cannot be recognized as an earthquake zone today. However, based on seismic sections on the northern flank of the STZ close to the Swedish coast, Gregersen et al. (1996) found signs of faulted sediments of presumably Lateglacial age. Based on these findings, the authors suggested that the deformation structures in the Quaternary sediments were the result of reactivation of the northern boundary fault of the STZ around the time of deglaciation. The observations, however, could not be confirmed by other types of data. The findings of Gregersen et al. (1996) were further accentuated by results from sequence stratigraphy, biostratigraphy and ^{14}C dating from the southern part of Kattegat, where deformed Lateglacial sediments associated with a NW-SE elongated depression were found (Jensen et al., 2002). The authors concluded that the deformations were caused by reactivation of faults in the Fennoscandian Border Zone between ~15 ka to 13.5 ka because of the Late Weichselian isostatic adjustment. The southern and eastern parts of Kattegat covered by the two examples mentioned above are within the part of the STZ with the highest intensity of historic earthquakes in Denmark (Gregersen and Voss, 2012).

Equally convincing examples of relationships between deformed Quaternary sediments, deep faults and earthquakes are scarce in the northwest segment of the STZ. The down-faulted

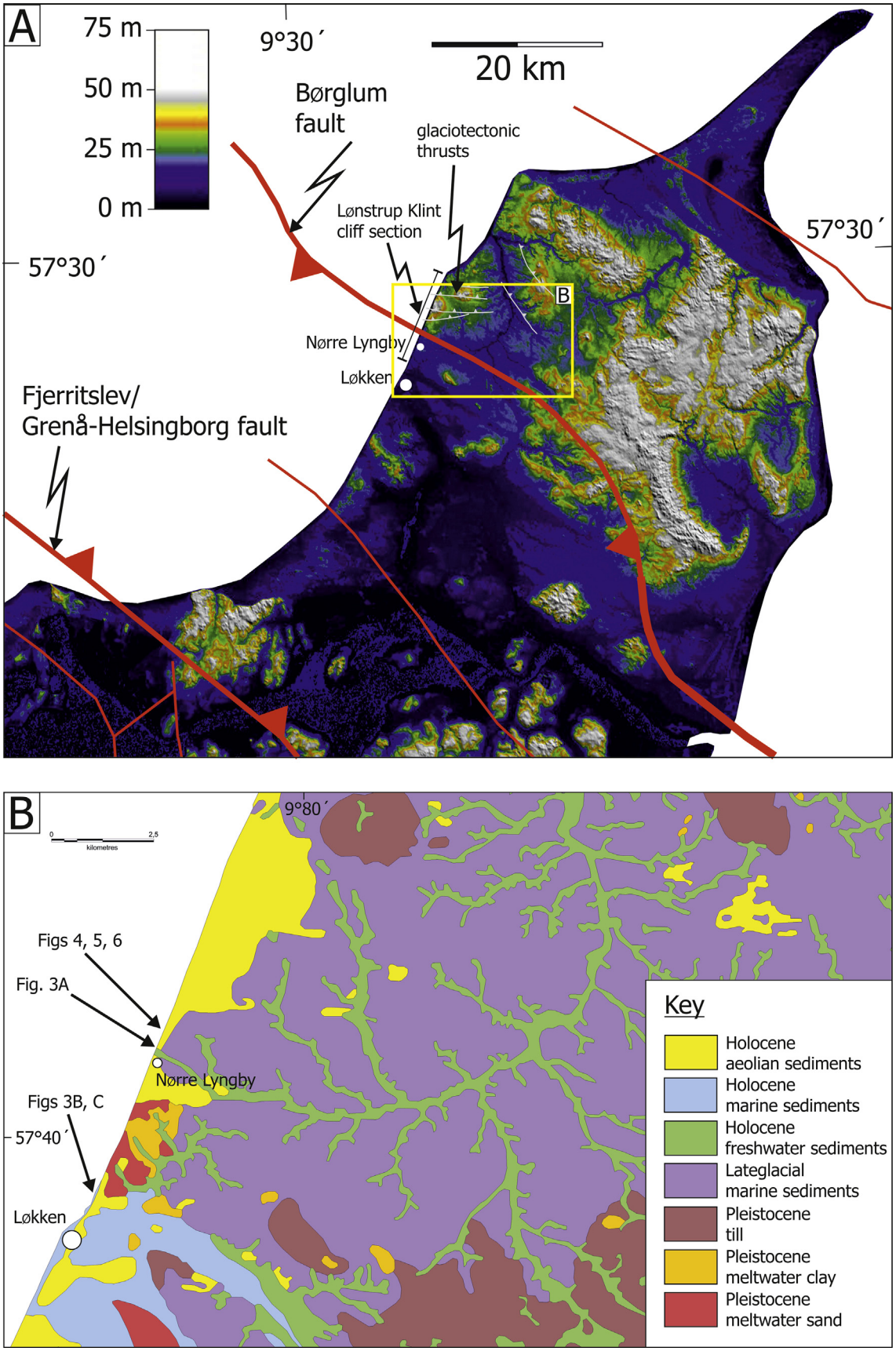

Fig. 2. A) DEM of the study area with mapped faults. The DEM is based on SRTM data (3 arc seconds). The faults are from Kley and Voigt (2008). The glaciotectonic thrusts in the area are based on Pedersen (2005) and are shown in grey. B) Geological map of the study area, based on Pedersen et al. (2011).

Lateglacial sediments in the Nørre Lyngby basin comprise the best example (Lykke-Andersen, 1992). Here, a listric fault with an offset of around 30 m was found underneath an elongated freshwater basin and the author suggested an earthquake as the triggering factor followed by gravitational creep. According to Lykke-Andersen (1992) the faulting took place in the period 12.500 to 11.800 years before present. However, this estimate was based on uncalibrated ^{14}C ages of lacustrine deposits. No association with specific deep faults was made by Lykke-Andersen in the 1992-paper, but a tentative association between the fault at Nørre Lyngby and movements of deep-seated faults of the STZ was made in an earlier paper (Lykke-Andersen, 1979). In the northern part of Denmark, Lykke-Andersen and Borre (2000) found, using 60 years of precise leveling data, signs of recent movements along the faults of the northwest segment of the STZ. But as mentioned by Gregersen and Voss (2012) the movements could be due to aseismic creep.

2.2. The geology of northern Jutland

2.2.1. Bedrock geology

Tectonic movements within the STZ have had great impact on the sedimentation and erosion since the Paleozoic. The top pre-Zechstein sub-crop consists of a Precambrian basement with Paleozoic sandstones and shales above, which form the remnants of a large sedimentary basin (Vejbæk and Britze, 1994). The top of the pre-Zechstein lies at depths of around 1–4 km north of the STZ, between 4 and 9 km inside the boundary faults of the STZ and at around 5–6 km just to the south (Vejbæk and Britze, 1994). At the end of the Paleozoic, erosion had created a peneplain, but reactivation of the STZ in the Early Triassic caused subsidence creating accommodation space for up to 6000 m thick sediments, which comprise sandstones, claystones and limestones (Britze and Japsen, 1991; Michelsen and Nielsen, 1991; Mogensen and Korstgård, 2003). Further subsidence in Jurassic to Early Cretaceous times took place primarily within the two main faults of the STZ (Mogensen and Korstgård, 2003) and the sediments from this period comprise clays and sands. The largest thicknesses can be found within the STZ ranging from 1000 m to 2500 m compared with 500–1000 m to the north (Japsen and Langtofte, 1991; Michelsen and Nielsen, 1991). The sedimentation of fine-grained chalk (limestone) in the Late Cretaceous and coarser grained carbonates in the Danian was largest in the central parts of the Danish Basin attaining thicknesses typically above 1500 m, whereas the thicknesses further to the north are less than 1000 m (Japsen and Langtofte, 1991).

The sediments from the Early Cretaceous to Danian form the Quaternary subcrop in the northern part of Denmark and it is estimated that around 1000 m of sediments have been eroded during the late Cenozoic (Japsen and Bidstrup, 1999). The pre-Quaternary surface has a general northerly dip from around sea level south of the study area to more than 250 m below sea level to the north (Binzer and Stockmarr, 1994). A local, structural low in the Top Chalk Group (Ter-Borch, 1991) is situated just south of the Børglum Fault.

2.2.2. Quaternary geology of the study area

During the Late Pleistocene Weichselian glaciation, northern Denmark was repeatedly covered by ice and large ice-dammed lakes formed in front of the ice sheets (Larsen et al., 2009; Böse et al., 2012). At the Lønstrup Klint a large glaciotectonic complex is exposed that formed during the last major ice advance at around 23–21 ka (Figs. 1 and 2B). This glaciotectonic complex comprises thrust sheets of Late Pleniglacial glaciolacustrine and glaciofluvial deposits (Lønstrup Klint, Kattegat Till and Ribjerg Formation) and is overlain by a till of the Mid-Danish Till formation (Sadolin et al., 1997; Houmark-Nielsen and Kjær, 2003; Pedersen, 2005; Houmark-Nielsen, 2007; Larsen et al., 2009).

Northern Denmark became ice-free after 19 ka and rapid marine inundation of the study area occurred (Krohn et al., 2009). Shallow-marine deposits of the Vendsyssel formation unconformably overlie parts of the glaciotectonic complex. These deposits were formerly referred to as Lower *Saxicava* sand, younger *Yoldia* clay, Upper *Saxicava* sand and *Zirphea* beds and range in age from approximately 18 to 12 ka (Lykke-Andersen, 1992; Houmark-Nielsen and Kjær, 2003; Richardt, 1996, 1998; Sadolin et al., 1997; Pedersen, 2005; Krohn et al., 2009; Larsen et al., 2009). The deposits formed under arctic to subarctic conditions during forced regression (Jessen, 1918, 1931; Richardt, 1996, 1998; Pedersen, 2005; Krohn et al., 2009), caused by the onset of glacio-isostatic uplift of the deglaciated areas (Richardt, 1996, 1998). The marine sediments of the Vendsyssel formation consist of an overall coarsening-upward succession commonly starting with fine-grained mud with dropstones (younger *Yoldia* Clay), deposited in an offshore environment during sea-level highstand. Estimated water depths are more than 20–30 m (Richardt, 1996; Pedersen, 2005). In a few places, at the base of the formation, up to 2 m thick coarse-grained sand and gravel with shell debris occurs that probably indicate deposition during transgression (Richardt, 1996; Pedersen, 2005). Upsection, the fine-grained offshore deposits are overlain by mud-sand couplets of the offshore-transition zone and thicker bedded shoreface sands. At the top, the Vendsyssel formation is bounded by an erosional unconformity and the sediments are locally overlain by Lateglacial to Holocene non-marine deposits and/or aeolian deposits (Jessen and Nordmann, 1915; Lykke-Andersen, 1992; Krog, 1978; Sadolin et al., 1997; Pedersen, 2005; Fischer et al., 2013). These deposits occur in several small depocenters that trend E-W, WNW-ESE and NW-SE and are exposed along the Lønstrup Klint cliff. One of these depocenters is represented by the Nørre Lyngby basin, where at least 15 m thick lake deposits have been accumulated. The lake deposits of this fault-bound basin contain important late Palaeolithic artifacts, which record some of the northernmost traces of human presence in Northwestern Europe during the Lateglacial (e.g., Jessen and Nordmann, 1915; Fischer et al., 2013 and references therein).

South of Nørre Lyngby, Holocene marine deposits of the Littorina transgression are exposed in a larger NW-SE trending depocenter (Fig. 3). The Littorina clay overlies Holocene freshwater deposits (Jessen, 1936; Penney, 1985). Apart from areas with these local occurrences of Lateglacial to Holocene sediments, the top of the Vendsyssel formation constitutes the terrain surface in a large part of western Vendsyssel (Fig. 2B).

3. Results

3.1. Outcrop data

Our study area is the Lønstrup Klint cliff at the northern coast of Denmark facing the Skagerrak. A detailed structural analysis was carried out for a cliff section, located at N57°24′57.8"/ E009°44′53.3", north of Nørre Lyngby. This section (Fig. 4) is approximately 12 m high and 50 m long. It exposes shallow marine sediments of the Vendsyssel formation (younger *Yoldia* clay and upper *Saxicava* sand) that are unconformably overlain by lacustrine

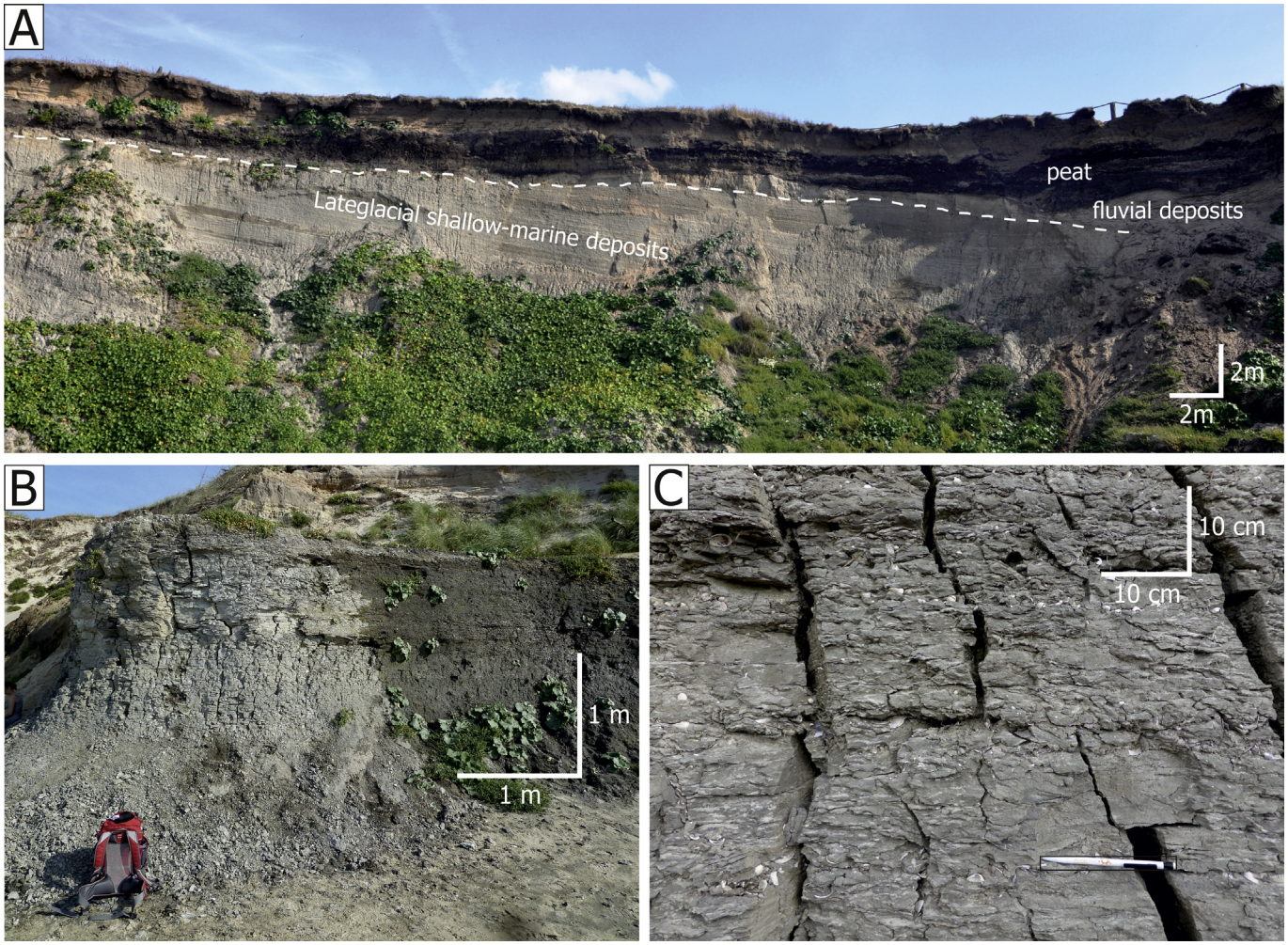

Fig. 3. Young Lateglacial to Holocene fault-related mini-basins filled with marine and freshwater deposits. A) Mini-basin that extends north and south of the Nørre Lyngby beach driveway (Nørre Lyngby vej). Tilted Lateglacial shallow-marine deposits (younger *Yoldia* clay) are unconformably overlain by freshwater deposits. B) Mini-basin north of Løkken filled with Holocene marine deposits (*Littorina* clay). C) Close-up view of B) showing marine mud with shell layers.

and aeolian deposits (Jessen and Nordmann, 1915; Lykke-Andersen, 1992; Sadolin et al., 1997; Richardt, 1998; Pedersen, 2005; Fischer et al., 2013).

The basal sedimentary succession gently dips towards NNE and consists of a shallowing-upward sequence of offshore-transition to shoreface deposits. ^{14}C ages range between ~14.5 and 14.1 ka (Richardt, 1998). These marine forced regressive deposits are unconformably overlain by steeply to gently dipping medium-to thick-bedded sand and pebbly sand with wave-ripple cross-lamination, climbing-ripple cross-lamination and trough cross-stratification, indicative of a lacustrine deltaic environment (e.g., Lang et al., 2015). These deltaic sands partly contain thin peat layers and are Older Dryas or Allerød in age (~14.5 ka, Fischer et al., 2013). They are overlain by organic-rich clay and thin-bedded sand-mud couplets, indicating a decrease in detrital input in a probably deeper low-energy environment. The age of these deposits is Allerød (Fischer et al., 2013). Within this succession many mainly WNW-ESE and E-W trending planar normal faults (Fig. 4) are developed. The displacement is in a range of centimeters to decimeters (Figs. 4 and 5), but one fault shows a displacement of approximately 3 m (Fig. 6). Most of the normal faults are post-depositional and form conjugate patterns (Fig. 4). The faults can be seen at different stratigraphic levels (Fig. 4). At one of these faults, syntectonic wedge-shaped growth strata are developed in the marine deposits, with the greatest sediment thickness close to the fault plane (Fig. 5G and H). Some of the faults are developed as tabular shear zones and represent deformation bands (cf. Fossen et al., 2007; Brandes and Tanner, 2012; Brandes et al., 2018). Kristensen et al. (2013) presented a detailed study on the shear bands exposed at Nørre Lyngby.

The sediments that were affected by faulting also show several meta- and postdepositional soft-sediment deformation structures (Fig. 5B, C, D, E). These are ball-and-pillow structures and associated flame structures. The ball-and-pillow structures reach up to 20 cm in diameter. Pillows commonly have a lenticular, concave-up shape and are developed in sand-mud couplets, whereas the more ball-like structures occur in thicker, probably storm-derived, sand beds (Fig. 5E). The flame structures have triangular and partly spear-like geometries with heights of 5–20 cm. They consist of sand to mud and are intruded into sand or sand-mud couplets. They are mostly vertical; in some cases, they are inclined. The flame and ball-and-pillow structures are partly associated with diffuse fluidized zones. At the base of the section, some of the ball-and-pillow structures are offset by normal faults (Fig. 5B).

These deformed marine and lacustrine sediments are onlapped and overlain by undeformed subhorizontally bedded lacustrine sand-mud couplets with wave-ripple cross-lamination that are Younger Dryas in age (Fischer et al., 2013). Upsection these sand-

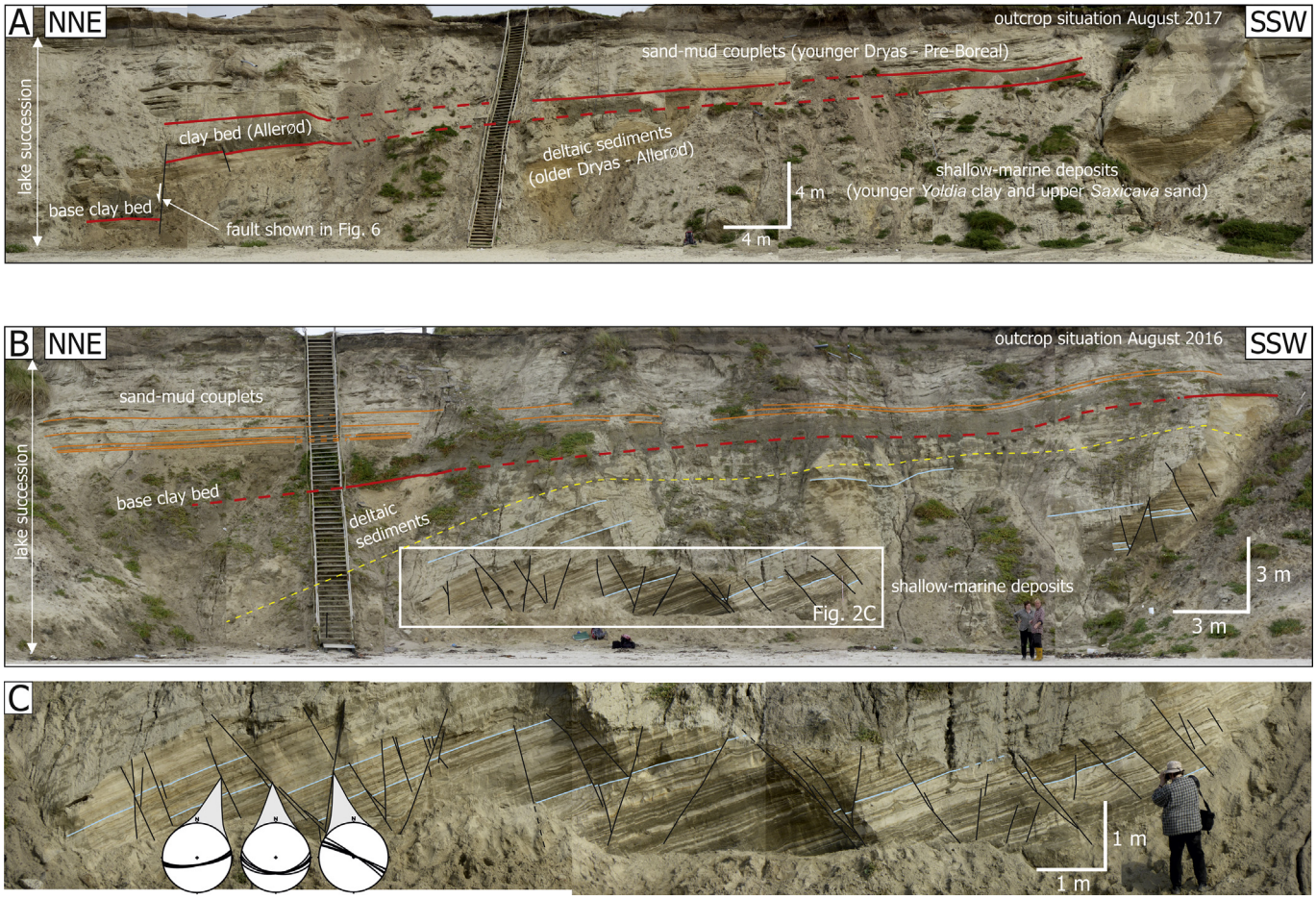

Fig. 4. Photo panel of the cliff section, showing the depositional architecture of the Nørre Lyngby basin. A) Exposure conditions 2017, B) Exposure conditions 2016. C) Close-up view of B) showing a normal fault array.

mud couplets pass into more sand-rich shallow lake sediments that were deposited during the Younger Dryas to Pre-Boreal. At the top, the lake sediments are bounded by an unconformity and are overlain by Holocene aeolian deposits.

Along a normal fault with 3 m displacement (that offsets the organic-rich clay bed), hydrofractures are developed that are rooted in the fault and propagated into the host sediment (Fig. 4A; 6).

3.2. Interpretation

Selsing (1981) and Meier and Kronberg (1989) showed that faults in unconsolidated sediments can be caused by tectonic or gravitational stress. We rule out recent gravitational deformation in the cliff because most of the faults trend almost perpendicular to the cliff face. If they were caused by gravitational forces they should trend parallel to the cliff face (e.g., Brandes and Winsemann, 2013). We also rule out compaction, because one of the exposed normal faults has an displacement of 3 m. This localized high displacement cannot be explained by compaction effects. Also, most of the faults follow the trend of the Børglum fault in that area (Figs. 4 and 5). Comparable dense sets of normal faults have been interpreted as seismites (Seilacher, 1969; Anand and Jain, 1987; Ringrose, 1989).

Ball-and-pillow structures and flame structures mainly indicate liquefaction processes, caused by sand sinking into water-saturated fine-grained sediments (Lowe, 1975; Owen, 1996; French, 2007; van Loon, 2009; Brandes and Winsemann, 2013). Associated diffuse fluidized zones suggest that fluidization developed locally within the lower layer and that deformation driven by water escape was superimposed on deformation driven by the gravitationally unstable density gradient (Owen, 1996; Brandes and Winsemann, 2013).

There are various trigger mechanisms that can cause such soft-sediment deformation structures in a shallow marine or lake environment including earthquakes, depositional loading or storm waves (e.g., Rossetti, 1999; Alfaro et al., 2002; Owen and Moretti, 2011; Chen and Lee, 2013). Storm events in marine shoreface or shelf-shoreface transition zones may trigger liquefaction and fluidization by i) overloading during rapid sedimentation of storm beds; ii) the direct impact of breaking waves or iii) cyclic stresses caused by pressure differences between the crests and troughs of wave trains (e.g., Alfaro et al., 2002; Chen and Lee, 2013). However, as these structures are restricted to the faulted succession we find that seismic shock waves are the most likely trigger mechanism for the observed soft-sediment deformation structures. This is supported by the occurrence of large hydrofractures (Fig. 6). These hydrofractures indicate a strong fluid pressure increase (Phillips et al., 2013; Phillips and Hughes, 2014; Lee et al., 2015). Comparable sand-filled fractures were interpreted to have formed during earthquakes (e.g., Hatcher et al., 2012).

A small growth package that is developed at one of the normal faults (Fig. 5 G, H) points to sedimentation during fault movement. The continuous thickness increase of the sediments may indicate fault creep.

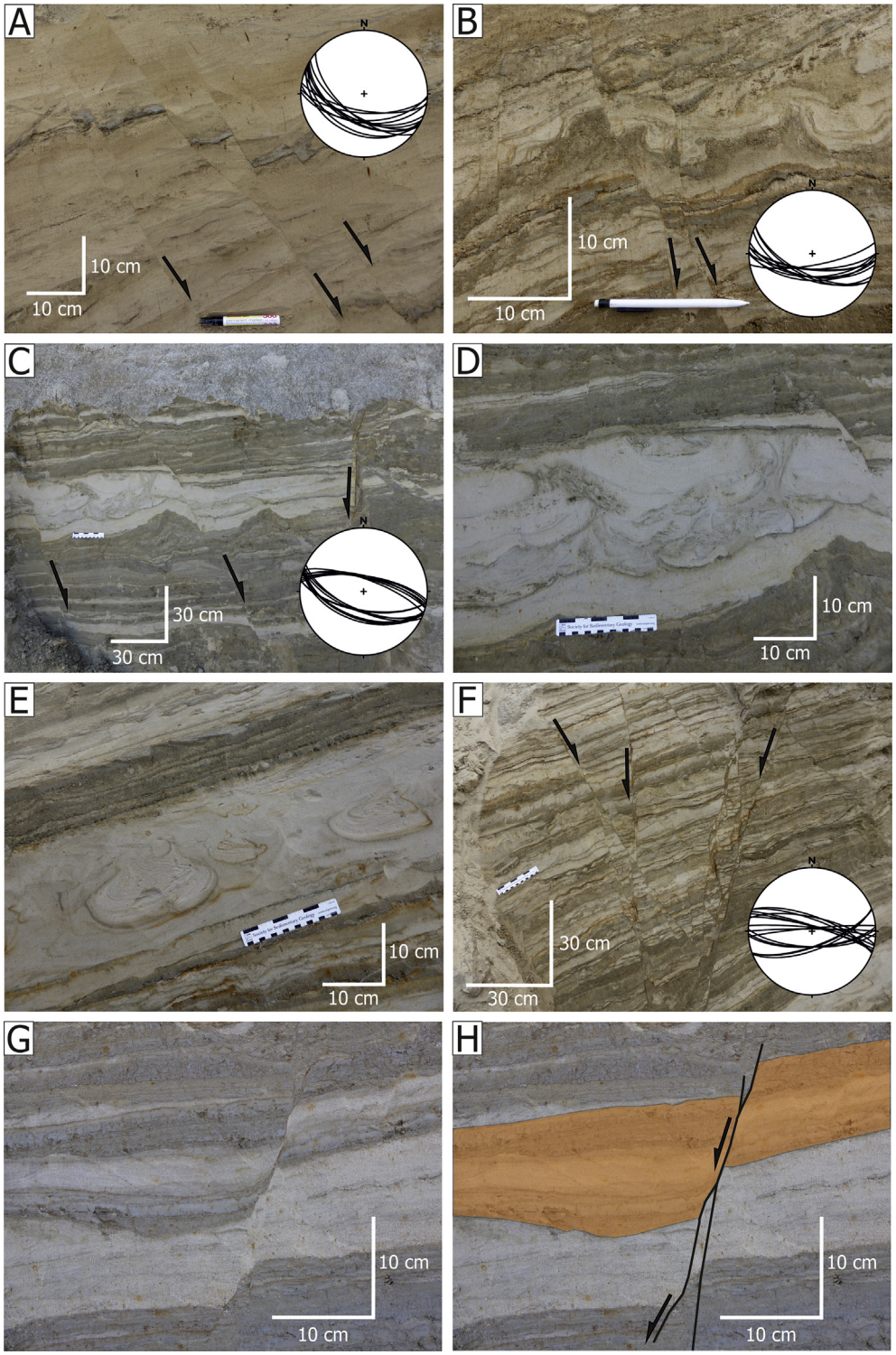

Fig. 5. Faults and soft-sediment deformation structures in the analysed outcrop at the Lønstrup Klint section. The stereographic projections show the orientation of the exposed faults. A) Planar to slightly curved normal faults developed in Lateglacial (Older Dryas or Allerød) lacustrine deltaic sediments. B) Soft-sediment deformation structures that are offset by curved normal faults. C) meta-depositional soft-sediment deformation structures in Lateglacial shallow-marine sediments that are offset by postdepositional conjugate normal faults. D) Close-up view of C) showing the truncated metadepositional soft-sediment deformation structure. E) Postdepositional ball- and pillow-structures in Lateglacial shallow-marine sediments. F) Conjugate set of normal faults. G) Normal fault with wedge-shaped growth strata in Lateglacial shallow-marine sediments that indicate syn-sedimentary fault activity. H) Growth-strata highlighted in yellow. (For interpretation of the references to colour in this figure legend, the reader is referred to the Web version of this article.)

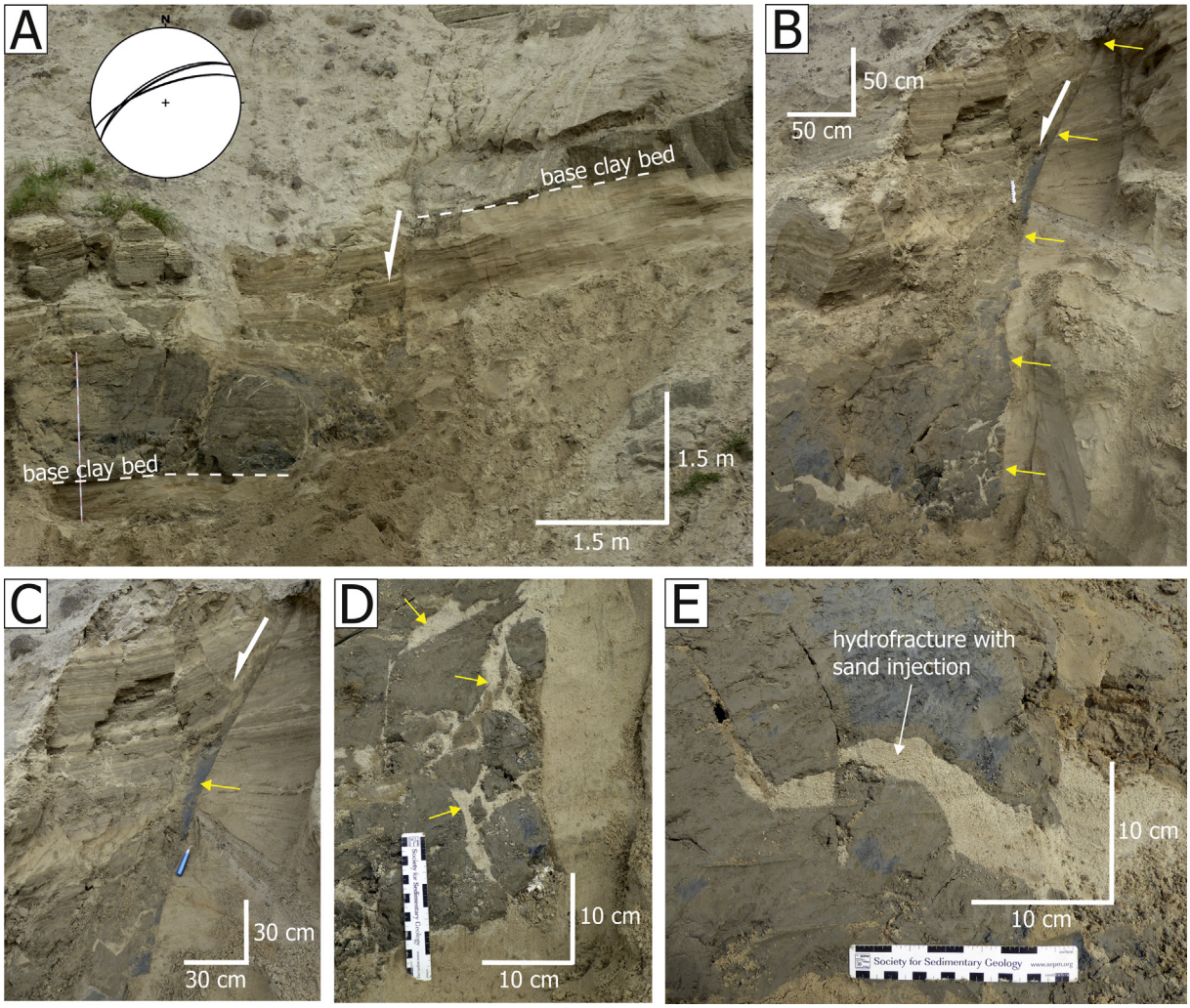

Fig. 6. Normal fault and hydrofacturing features developed in Lateglacial lacustrine deposits. A) Large normal fault that offsets an Allerød clay bed with a displacement of 3 m (see also Fig. 4A). B) Detail of the fault. The yellow arrows indicate the fault trace. C) Clay smear (indicated by the yellow arrow) developed along the fault plane. D) Sand filled hydrofractures (indicated by the yellow arrows) that developed in the Allerød clay bed. The extensive development of hydrofractures is interpreted as the result of fluid-overpressure, caused by seismic shockwaves. E) Detail of a sand-filled hydrofracture.

The occurrence of syn- meta- and postdepositional soft-deformation structures at different stratigraphic levels point to a series of seismic events that occurred approximately between ~14.5 and ~12 ka (Fig. 5B, D, E).

3.3. Topographic analysis in the Nørre Lyngby area

The terrain surface in the area east of the cliff section is dominated by the Lateglacial marine sediments. At some places remnants of meltwater deposits occur that form isolated hills and in topographic lows, Lateglacial and Holocene freshwater and marine sediments form the top of the terrain. Holocene aeolian sediments form a narrow belt along the coastal cliff (Fig. 2B; Pedersen et al., 2011). The coloured interval map in Fig. 7A shows the topography in the Nørre Lyngby area based on LiDAR data with a vertical resolution of ~0.15 m and with a horizontal discretization of 1.6 m. The LiDAR data were handled in ArcMap and rasterized using inverse distance-weighted interpolation. The colour-coded interval map shows coloured intervals and intervening white intervals each representing an altitude change of 1 m. The colouring is chosen arbitrarily to visually enhance the topographical changes and the sequence is repeated every 10 m with increasing colour intensity with increasing altitude.

The erosional pattern is highly segmented and to analyse the overall pattern in the area individual segments of linear erosional features have been vectorised in MapInfo Pro (Fig. 7B). The vectorisation focusses on linear erosions/depressions that exceed 200–300 m, although shorter vectors have been used locally, when vectorising parts of longer depressions. In Fig. 7B the interval colours are diminished to make the annotations more visible. A total of 354.1 km of erosional segments has been digitized. The vector data were extracted from MapInfo using GeoMapVector and the rose diagram (Fig. 7C) was made using GeOrient 9 (Rod Holcombe, Australia). The rose diagram is made as a length azimuth plot with the accumulated lengths of the vectors plotted within 5-degree intervals. No filtering or moving average has been applied.

3.4. Interpretation

The rose diagram in Fig. 7C shows a pronounced dominance of erosional valleys with WNW-ESE to NW-SE orientations (A on Fig. 7C) and with less dominant orientations around W-E (B on Fig. 7C), N-S (C on Fig. 7C) and WSW-ENE (D on Fig. 7C). The dominant orientation covers a rather broad interval suggesting two

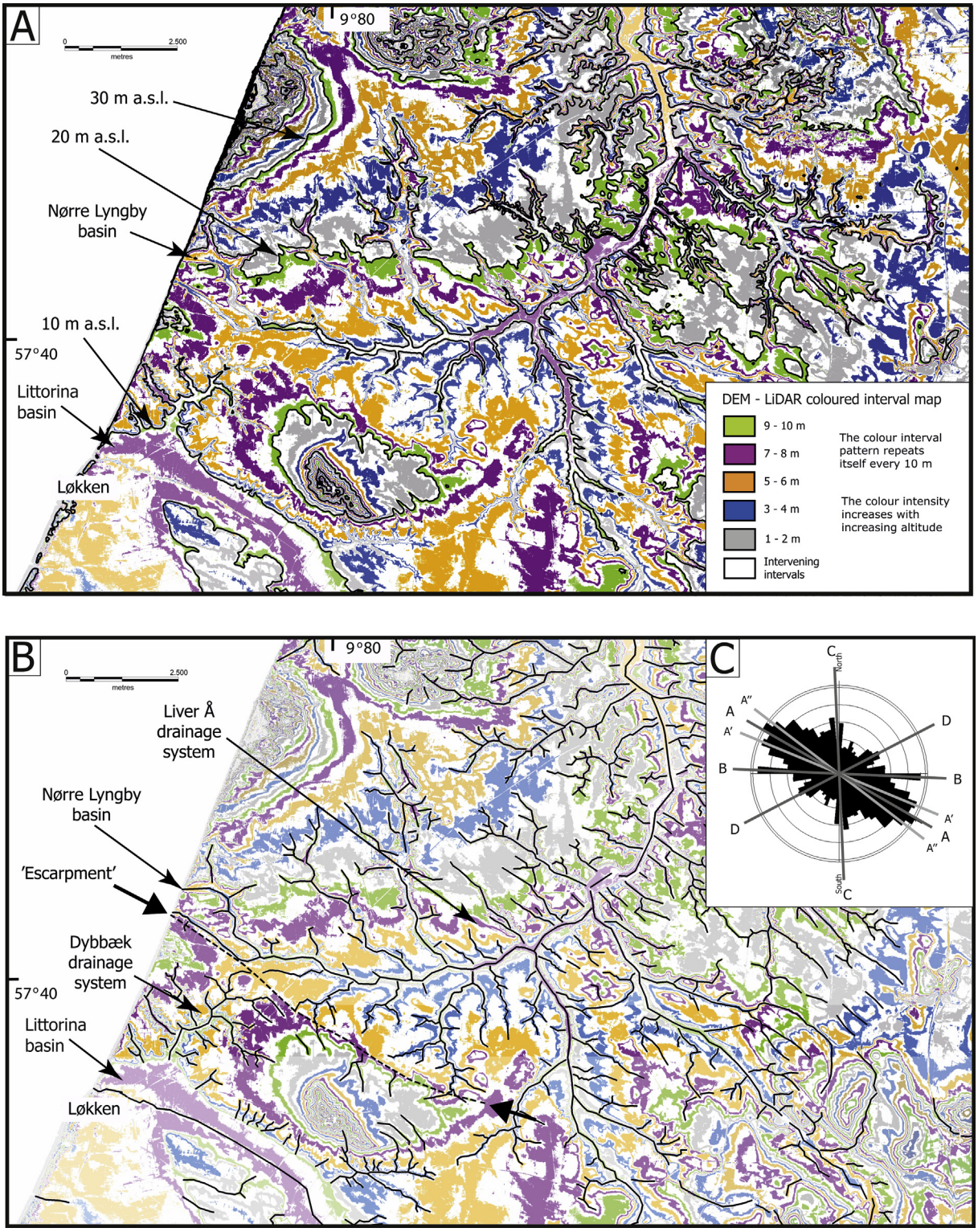

Fig. 7. Topographic analysis. A) Digital elevation model (DEM) based on LiDAR data presented as a coloured interval map. Contours of 10, 20 and 30 m a.s.l. are highlighted with black lines. B) Erosional valleys in the topography digitized as vectors along the valley bottom. A WNW-ESE 'escarpment' of 1–2 m height is shown as a hatched line highlighted with arrows. On either side of the escarpment, the Liver Å (brook) has a drainage in northeastern to northern direction and the Dybbæk (brook) in a southwestern direction, respectively. C) Rose diagram showing cumulated lengths of lineaments from Fig. 7B plotted in 5-degree petals. Highlighted orientations marked with grey lines represent inferred dominant orientations (see text).

separate populations of WNW-ESE (A′ on Fig. 7C) and NW-SE (A″ on Fig. 7C), respectively.

The study area has two separate drainage systems: the dominant system of the stream Liver Å that drains most of the area in a northeastern to northern direction and a smaller system of the stream Dybbæk that drains a small area northeast of Løkken in a south-westerly direction (Fig. 7B). It is remarkable that the overall directions of the drainage in the two systems are perpendicular to the dominant orientation of the erosional pattern (Fig. 7C; rose diagram). The water divide between the two drainage systems is rather sharp and linear (see bold arrows in Fig. 7B) and appears as a subtle escarpment with the top of the marine sediments to the SW being 1–2 m higher than towards NE. The drainage patterns in the two areas share approximately the same orientations, but the erosional intensity is very different. The drainage systems meet along the lineament and with only slight erosional overlaps between the two the drainage systems appear to have been separated long time ago.

The pattern of preferred orientations of the erosional valleys as depicted by the rose diagram (Fig. 7C) points to an influence from structures within the sediments rather than an influence from the overall direction of the drainage. The dominant WNW-ESE to NW-SE orientation of the erosional valleys in the study area is comparable to earlier topographical analyses for all Vendsyssel (Sandersen and Jørgensen, 2002, 2016). These studies were based on less detailed data but showed that the erosional valleys had a preferred trend around WNW-ESE to NW-SE regardless of the terrain being of Late Pleniglacial, glacigenic or Lateglacial and Holocene marine deposits . As this orientation interval also matches the known deep faults in the area the authors concluded that tectonic movements related to deglaciation apparently had created deformed zones in the sediments all the way to the land surface. These more easily erodible deformed zones were likely to have controlled the drainage in Lateglacial and Holocene times (Sandersen and Jørgensen, 2016). Apparently, the pattern of the preferred orientations of Vendsyssel can also be found in the smaller Nørre Lyngby area.

Although the rose diagram (Fig. 7C) shows an overall pronounced orientation of the erosional valleys, it is obvious that the data contain multiple populations. In both the present study and in the earlier studies of the topography mentioned above, the Lateglacial marine terrains have a distinct W-E population of erosional valleys. The depression above the Nørre Lyngby basin forms part of the drainage system of the Liver Å (Fig. 7B) and it seems to be constrained by the same physical architecture as the rest of the fluvial drainage systems in a large part of Vendsyssel. The geomorphology of the study area is therefore interpreted to be strongly influenced by subsurface faults. As the erosional pattern lines up with the dominant orientation of the faults in Vendsyssel an impact from deeper tectonic structures is highly likely.

3.5. Modelling of the glacially induced fault reactivation potential

To analyse the potential connection between the decay of the Late Pleistocene ice sheets in northern Europe and the tectonic activity at the Børglum fault discussed above, we carried out three-dimensional finite element simulations that describe the process of glacial isostatic adjustment (GIA) together with those of Coulomb failure stress (CFS) calculations. The GIA models are based on the technique described in Wu (2004), Steffen et al. (2006) and Brandes et al. (2012) and allow testing of the reactivation potential of the Børglum fault due to GIA. Compared to our previous numerical studies (Brandes et al., 2012, 2015) we apply a few modifications. Horizontal element length is set to 50 km to accommodate new ice history model generations of similar spatial resolution and increase numerical accuracy of the results. Vertical layering is finer (5 km) in the upper crustal parts up to 30 km depth together with layer-dependent material parameters to retrieve a higher stress resolution than in our previous studies. We test models with and without lateral heterogeneities in the subsurface. Laterally homogeneous models have lithospheric thicknesses of [90, 140] km, upper mantle viscosity of [5, 8] x 10^{20} Pa s and lower mantle viscosity of 2 × $10^{[21, 22]}$ Pa s. These values are based on recent GIA studies for Fennoscandia (Lambeck et al., 2010; Zhao et al., 2012; Kierulf et al., 2014). Laterally heterogeneous models use a three-dimensional (3D) mantle viscosity structure converted, using the method by Wu et al. (2013), from the seismic tomography model by Grand et al. (1997). We adopt the 3D viscosity structure used by Kierulf et al. (2014). We connect this structure to models with 90 and 140 km lithospheric thickness, respectively. Finally, the characteristic change in

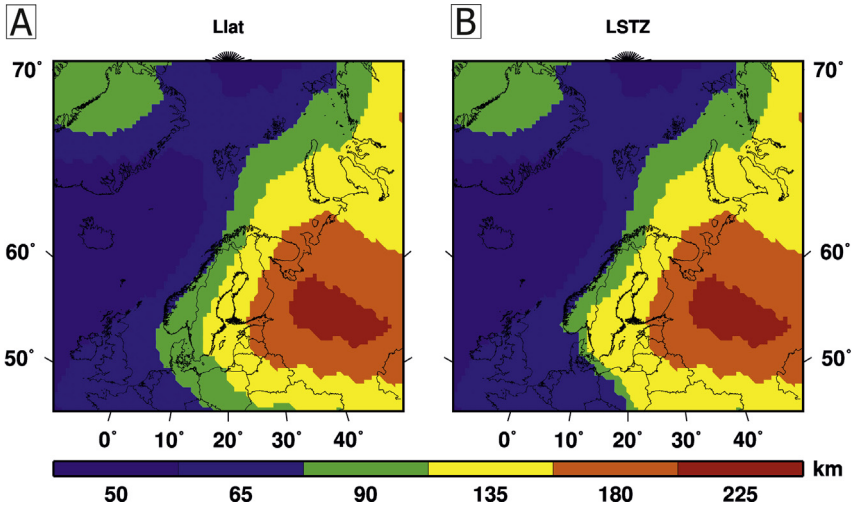

Fig. 8. Lithosphere models that serve as input for the GIA simulations. The thickness is colour-coded. A) Standard lithosphere model Llat. B) Manually modified lithosphere model LSTZ where a sharper lithosphere thickness increase over a short distance along the STZ was implemented. (For interpretation of the references to colour in this figure legend, the reader is referred to the Web version of this article.)

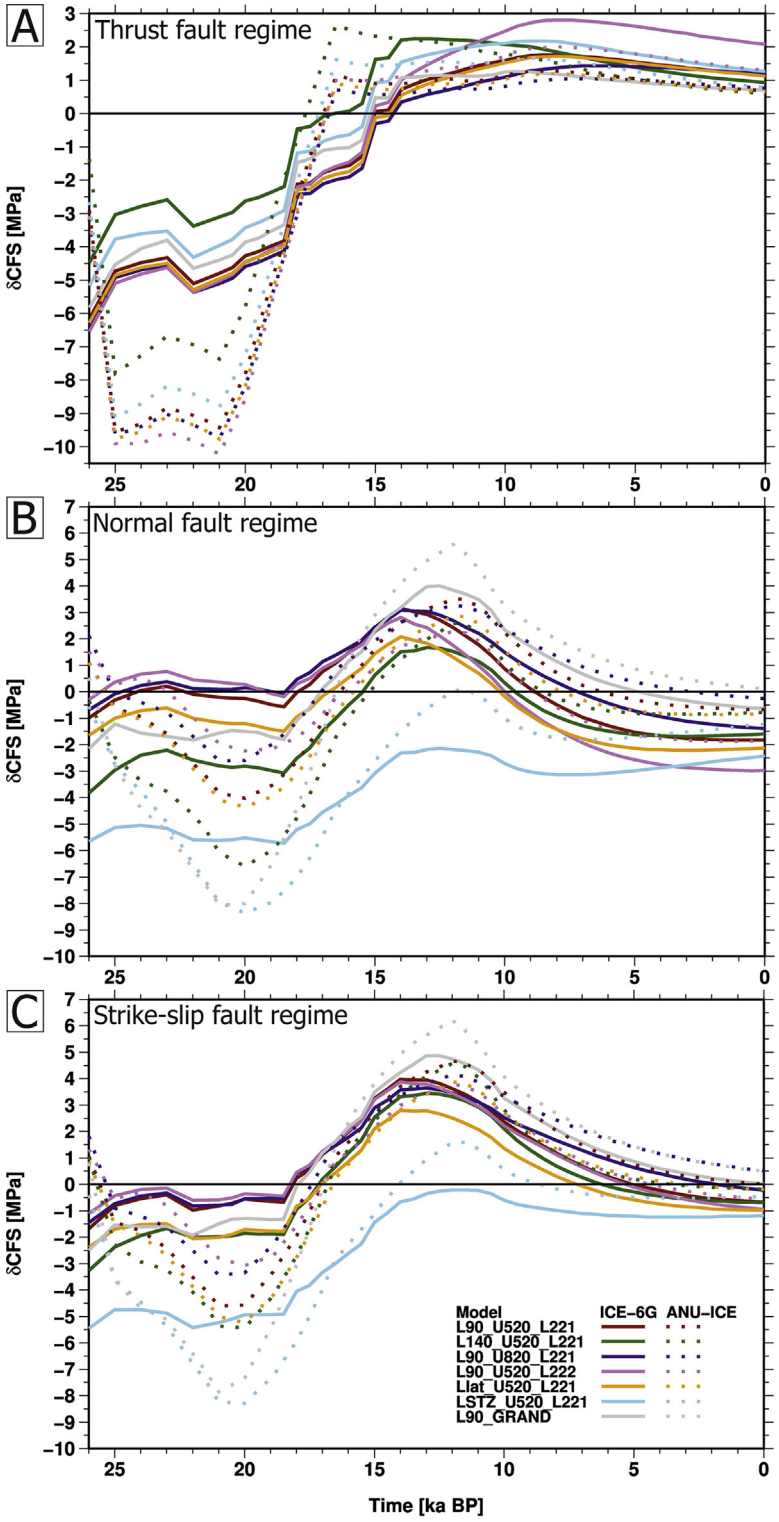

Fig. 9. Modelling results with the development of the Coulomb failure stress in the study area over the last 26 000 years. The simulation was performed with two different ice history models. The solid lines represent the results for the North-European part of the global ice model ICE-6G_C (Argus et al., 2014; Peltier et al., 2015). The second ice history model (dashed lines) is a combination of the ANU-ICE ice history models for the British Isles (Lambeck, 1995) and Fennoscandia (Lambeck et al., 2010). The convention for naming the models is as follows: the first L is the lithospheric thickness being 90 or 140 km, or one of the laterally varying models (lat, STZ) shown in Fig. 8; U is the upper-mantle viscosity with 5×10^{20} [520] or 8×10^{20} [820] Pa s; the second L is the lower-mantle viscosity with 2×10^{21} [221] or 2×10^{22} [222] Pa s; GRAND represents a laterally varying upper and lower-mantle viscosity model. See text for more information.

lithosphere thickness at the STZ was implemented into the models to provide a realistic representation of the lithosphere structure and to test this effect on the reactivation potential (Fig. 8). We apply two different structures; the structure in Fig. 8A, named Llat, is derived from the global lithosphere model introduced by Wang and Wu (2006), while the second in Fig. 8B, named LSTZ, is a manually updated version of Fig. 8A with a sharper contrast at the STZ. We note that LSTZ is for test purposes only to examine how such a sharp contrast as indicated in teleseismic tomography investigations by Cotte et al. (2002) would affect the CFS. The two 3D lithosphere models are combined with the mantle viscosity values above but not with the 3D mantle viscosity model.

We apply two different ice history models. The first is the North-European part of the global ice model ICE-6G_C (Argus et al., 2014; Peltier et al., 2015) which is available for the last 26 ka BP in time steps of 500 years. We add another glaciation cycle as a simple sawtooth from 216 to 126 (full load) to 116 ka BP (load-free) as it was shown that such cycle increases the result accuracy (Johnston and Lambeck, 1999; Kaufmann et al., 2002; Kaufmann and Wu, 2002; Root et al., 2015). The load applied at 116 ka BP increases linearly until 26 ka BP. More detailed modelling of the glaciation changes before 26 ka BP does not affect our results. The second ice history model is a combination of the ANU-ICE ice history models for the British Isles (Lambeck, 1995) and Fennoscandia together with the Barents and Kara seas (Lambeck et al., 2010). This model spans the last 240 ka BP (thus two glaciation cycles) in varying time steps of at least 3 years and at maximum 45 000 years.

For the location Nørre Lyngby, we calculated the change in CFS (δCFS, see Brandes et al., 2015 for details) for all three stress regimes: compressional, extensional and neutral (strike-slip) (Fig. 9). All three regimes are tested because the overall tectonic background stress regime is compressional (acting in NW-SE direction) but strike-slip behavior (common in a neutral regime) has been identified along the Børglum fault. Moreover, small (near-surface) normal faults (that develop due to extensional processes) are present along the cliff section, although these can likely be related to the development of the Nørre Lyngby basin. We assume a stress difference of 10 MPa between maximum and minimum background stress, which is reliable based on earlier studies (Stein et al., 1989; Wu and Hasegawa, 1996a; b). Glacially induced stresses can easily exceed 10 MPa (Stein et al., 1989; Wu, 2004; Lund et al., 2009) and change the stress regime at a selected location. The δCFS represents the minimum stress required to reach faulting. A negative δCFS value indicates that the fault is stable, while a positive value means that GIA stress is potentially available to induce faulting or cause fault instability or failure unless released temporarily by an earthquake. Thus, $\delta CFS = 0$, i.e., the zero line in Fig. 9, is an indication of the onset of fault motion.

We show in Fig. 9 the δCFS at the Børglum fault for a commonly used GIA model applying ICE-6G_C ice history with an Earth model of 90 km lithospheric thickness, upper-mantle viscosity of 5×10^{20} Pa s and lower mantle viscosity of 2×10^{21} Pa s. We also add curves for selected tested Earth and ice model combinations that envelope the spread of δCFS results. In a compressional regime (Fig. 9A), the zero line is crossed mainly between 16.6 ka and 14.3 ka for the ICE-6G_C ice model and between 17.7 ka and 16.8 ka for the ANU-ICE ice model, suggesting that the fault was activated by the deglaciation process. In an extensional regime (Fig. 9B), most models show the onset of positive values between 15 and 18.5 ka, which, if not released, can last until today for certain models. The results for the neutral regime (Fig. 9C) exhibit a similar behavior as for the extensional regime. Remarkable for the latter two regimes is (i) that maximum positive values of δCFS are found between 11 and 14 ka and (ii) that our manually manipulated model with a sharp lithospheric thickness increase along the STZ yields the smallest δCFS value for ANU-ICE but the fault remained stable for ICE-6G_C during this period. Based on the analysis of all three regimes, we strongly suggest classifying the Børglum fault as glacially induced fault.

4. Discussion

Lykke-Andersen (1992) combined a seismic line with the cliff section along the Lønstrup Klint and interpreted an exposed synform as hanging wall deformation above a listric normal fault that soles out into a horizontal detachment at a depth of 45 m (see also Fischer et al., 2013). Based on uncalibrated ^{14}C ages, the fault activity was estimated to have occurred in the time interval ~12.5–11.8 ka B.P and Lykke-Andersen stated that this fault formed as a consequence of an earthquake. New calibrated ^{14}C ages of the Vendsyssel formation and the Lateglacial lake deposits point to a slightly older fault activity at around ~14.5 to 12 ka (e.g., Richardt, 1998; Krohn et al., 2009; Fischer et al., 2013). Kristensen et al. (2013) postulated four potential drivers for the observed faulting: a) glacial rebound of the area, b) reactivation of the Børglum and Fjerritslev faults, c) outwash of clays or d) differential compaction.

The observed syn- meta- and postdepositional soft-sediment deformation structures (Fig. 5B, D, E) clearly support the idea of earthquakes in this area. A strong argument for a co-seismic evolution of these features are the observed hydrofractures in the Lateglacial lacustrine sediments (Fig. 6), which link the faults and the soft-sediment deformation structures. These hydrofractures give evidence for an abrupt increase in fluid pressure (cf. Phillips et al., 2013; Phillips and Hughes, 2014; Lee et al., 2015) and the fact that they are rooted in one of the major faults exposed in the outcrop, indicates that the fluid pressure change was very likely earthquake-related.

Soft-sediment deformation structures commonly occur in the epicentral region (Papadopoulos and Lefkopoulos, 1993). The epicentral region is the area with the maximum earthquake intensity (Davison, 1921). This implies that the epicentre of the earthquake that caused the soft-sediment deformation structures exposed at the Lønstrup Klint cliff was nearby. The observed ball-and-pillow structures and flame structures indicate liquefaction and local fluidization processes, which can be used to estimate the magnitude of a seismic event (Galli, 2000; Rodríguez-Pascua et al., 2000; Berra and Felletti, 2011). The abundant liquefaction structures require magnitudes of $M_s \geq 4.2$ (Galli, 2000). The displacement of 3 m along one of the exposed faults (Fig. 6) may indicate even higher magnitudes of up to ~7 (cf. Wells and Coppersmith, 1994).

The nearest fault in the vicinity of the outcrop that can produce this magnitude is the Børglum fault (Figs. 1 and 2A). Pedersen and Gravesen (2010) also stated that the fault described in Lykke-Andersen (1992) developed above the Børglum fault. The onset of basin formation/subsidence must have started before the Older Dryas/Allerød (~14.5 ka), pre-dating the observed postdepositional deformation structures. There are some syn- and meta-deformational structures within the marine succession, which indicate this early fault movement and associated seismicity or at least fault creep. The deposition of relatively coarse-grained lacustrine delta deposits may reflect the climatic warming at the beginning of the Lateglacial, which has been recorded from various terrestrial records in Northwestern and Central Europe (e.g., Guiter et al., 2003; Iversen, 1973; Kasse et al., 2007; Turner et al., 2013; Meinsen et al., 2014; Wohlfarth et al., 2018). The overlying fine-grained organic rich lake-bottom sediments indicate a decrease in sediment supply that was probably associated with an increase in water depths, either related to an increase in fault-related subsidence or a climate-controlled lake-level rise during the Allerød,

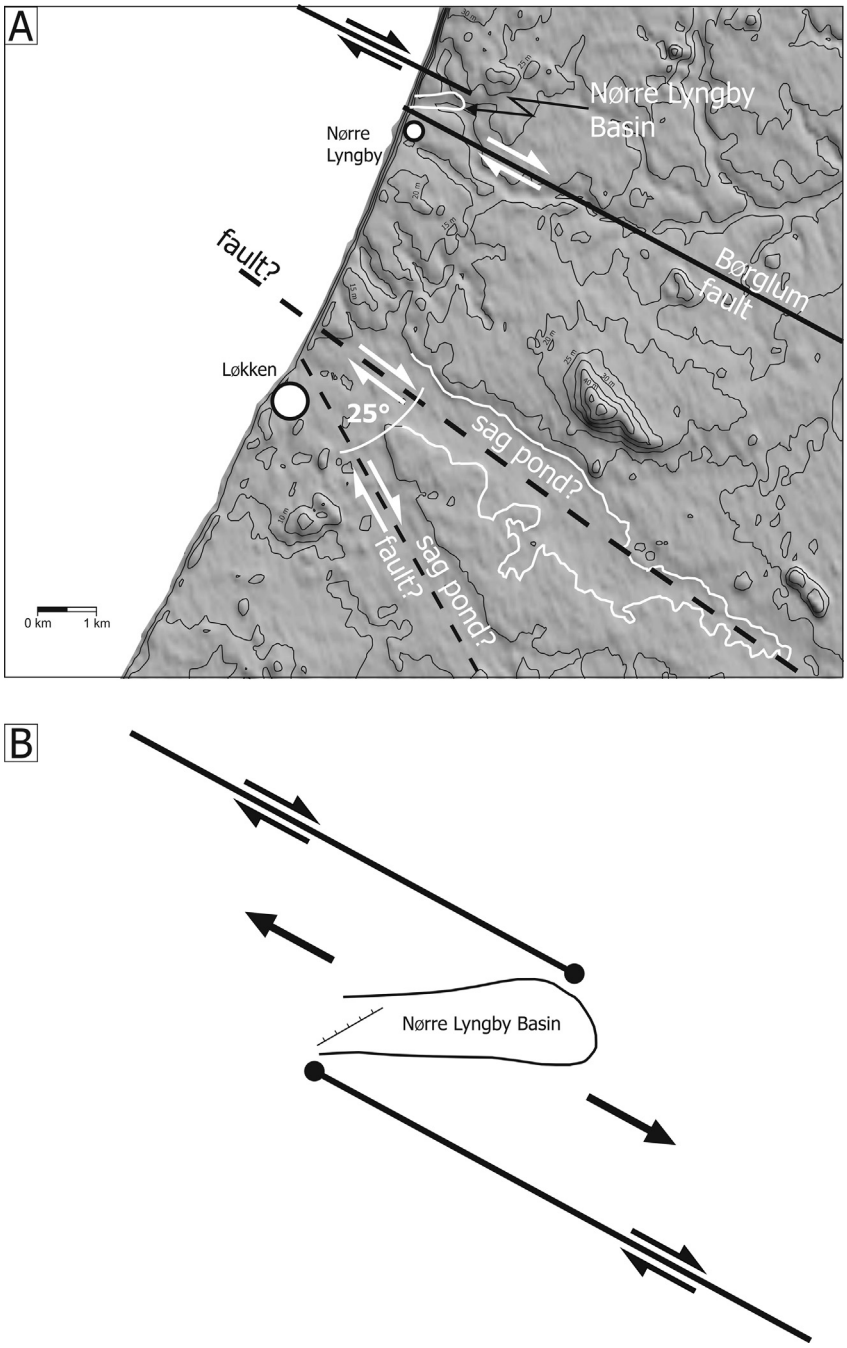

Fig. 10. Tectonic model. A) Detailed map and DEM of the area between the Børglum fault and Løkken. The Nørre Lyngby basin is interpreted as a small basin related to strike-slip movements of the Børglum fault (basin outline in white taken from Fischer et al., 2013). A strike-slip fault may explain the elongated valley east of Løkken possibly representing a kind of sag pond. The geometry of the elongated valleys east of Løkken resembles a fault with a related Riedel shear. B) Conceptual model for the evolution of the Nørre Lyngby basin. The basin axis trends E-W and the Børglum fault in this area is has a WNW-ESE trend. This obliquity of the basin axis to the Børglum fault implies that the basin formed in a fault step-over situation. This is supported by the trend of the major normal fault in the outcrop that is roughly ENE-WSW.

when the development of a stabilizing vegetation cover led to a decrease in erosion rates and an increase in peak discharge (cf. Vandenberghe, 2008; Wohlfarth et al., 2018). During the Younger Dryas to Pre-Boreal a shallowing-upward succession was deposited that resulted in the complete filling of the lake basin. The overall concentric basin-fill indicates a decrease in subsidence and tectonic activity. The occurrence of reworked aeolian sediments in the uppermost lake succession (Fischer et al., 2013) corresponds with the colder and dryer conditions with increasing erosion rates and a decrease in water discharge (e.g., Guiter et al., 2003; Kasse et al., 2007; Turner et al., 2013; Meinsen et al., 2014; Wohlfarth et al., 2018). The tectonic activity prevailed into the younger Dryas as indicated by the offset of the Allerød clay (Figs. 4 and 6) and the presence of a larger 1.2–2.4 m wide soft-sediment deformation structure within the younger Dryas lake deposits (Fischer et al., 2013). This feature was interpreted as a collapse structure by Jessen and Nordmann (1915).

4.1. Tectonic geomorphology

The Nørre Lyngby basin extends inland in an easterly direction for at least 700 m as verified by a series of boreholes (Knudsen, 1978). This E-W basin orientation matches both the overall E-W trend of the faults found in the basin sediments (see Figs. 4 and 5) and the depression in the present-day terrain above the basin (Fig. 7A). Jessen (1936) described the so-called Tvonnet Rende a few hundred meters north of the Nørre Lyngby basin. This approximately 150 m wide mini-basin is filled with Lateglacial marine sediments and cannot be clearly seen in the topography. However, the basin formation might be also tectonic in origin. South of the Nørre Lyngby basin, another mini-basin is exposed, which is filled with Lateglacial to Holocene fluvial deposits and peat.

The faults in the Nørre Lyngby basin cut through the Lateglacial marine sediments and occasionally through the Lateglacial lacustrine sediments above (e.g., Figs. 4–6). The marine Lateglacial sediments constitute the terrain surface in the major part of the Nørre Lyngby area (see Fig. 2B) and therefore it would be highly likely that faults can be seen in the terrain surface either directly as fault traces or indirectly as linear depressions or as a structural impact on the erosional patterns. Because of the unconsolidated nature of the sediments, explicit fault traces are not easily recognizable, but impacts from tectonic deformation on the erosional patterns, could reveal information on an impact from deeper structures (Sandersen and Jørgensen, 2016).

Surprisingly, the analysis of the erosional pattern shows that the dominant orientation does not follow the drainage directions either to the southwest or northeast but an orientation perpendicular to this. This could be dictated by WNW-ESE to NW-SE oriented Lateglacial shorelines. Beach ridges and for instance the WNW-ESE trending lineament separating the two drainage systems (see Fig. 7B) could be the remnants of a Lateglacial shoreline facing northeast. However, with several nearby islands of glacigenic deposits in the Lateglacial sea, it seems unlikely that near-shore structures in this area would have developed the observed regularity. With an orientation comparable to the Børglum fault, the drainage divide is more likely the surface expression of a reactivated fault in the STZ. The escarpment formed by the reactivated fault apparently divided the drainage of the young Lateglacial landscape in two parts.

The very regular erosional pattern in the present-day terrain is therefore interpreted to be highly influenced by tectonic deformation of the sediments. The tectonic movements created deformed zones in the sediments, which form apparently more easily erodible zones that controlled the drainage pattern in Lateglacial and Holocene times.

4.2. Post-glacial stress build-up and glacially induced faulting

According to ^{14}C data (Richardt, 1998; Fischer et al., 2013), the timing of the faulting at around ~14.5 to 12 ka implies a connection between the fault activity and the decay of the Scandinavian ice sheet. Numerical simulations provide the best way to test the impact of glaciations and fault activity (Wu and Hasegawa, 1996a; b; Wu, 1997, 1998; Wu and Johnston, 2000; Grollimund and Zoback, 2001; Hetzel and Hampel, 2005; Hampel and Hetzel, 2006; Turpeinen et al., 2008; Hampel et al., 2009; Hampel et al., 2010; Steffen et al., 2014a; b; c; Hampel, 2017).

The Børglum fault was below the Scandinavian ice sheet during the Late Weichselian (MIS 2). The paleogeographic maps of Larsen et al. (2009) and Hughes et al. (2016) indicate that the study area was free of ice at around 18 ka and the southeastern part of the STZ was deglaciated at around 16 ka. In the ANU-ICE model, the study area gets ice-free around 17.6 ka and the southeastern part of the STZ between 16.5 and 16 ka. ICE-6G_C shows ice-free conditions in the study area at 18 ka and in the southeastern part of the STZ between 15.5 and 15 ka. According to the numerical simulations the δCFS became (model-dependent) positive between 17.7 ka and 14.3 ka in a compressional regime (Fig. 9A) or between 18.5 ka and 5 ka in an extensional or neutral regime (Fig. 9B and C). All three regimes point to instability. This strongly suggests that the fault was reactivated by the deglaciation process and provides an answer to the fault activity driving forces speculated by Kristensen et al. (2013). The early onset of fault instability can be an effect of the short distance between the ice margin and the STZ, which we will further illuminate in the following.

The potentially earthquake-related soft-sediment deformation structures (Fig. 5) are developed in sediments that were deposited between approximately ~14.5 to 12 ka B.P. (Lykke-Andersen, 1992; Richardt, 1998; Krohn et al., 2009; Larsen et al., 2009; Fischer et al., 2013), indicating seismic events at that time. The time interval between the modelled onset of fault instability and the time point when seismic activity started, according to geological observations, is thus in good agreement. During that time, the modelling shows partly strong stress increase of more than 1 MPa per 500 years independent of the background stress regime. The results of models with lateral lithospheric thickness variation (orange and cyan lines in Fig. 9), including our manually manipulated one (STZ), fall within the given time intervals under thrust regime and are also bounded by model results without lateral heterogeneity in either lithospheric thickness or mantle viscosity. Under the normal or the strike-slip stress regime, the STZ lithospheric thickness variation model (Fig. 8b) struggles in explaining the earthquakes if the ice history is given by ICE-6G_C. At that time, we can therefore not relate the past seismic activity to the special lateral lithosphere structure (with a steep gradient in lithospheric thickness) of the STZ that we tested. Clearly, the ice history model needs to be well determined before conclusions on the Earth structure can be drawn with the help of geological observations.

Based on the dated faulted sediments and modelling-derived times of fault instability, our study gives evidence for reactivations of the Børglum fault between ~14.5 ka to 12 ka. We therefore classify the Børglum fault as a glacially induced fault. Its reactivation was probably accompanied by distinct earthquakes of at least $M_S \geq 4.2$. Even higher magnitudes of up to ~7 (cf. Wells and Coppersmith, 1994) may be indicated by a fault with 3 m displacement in the outcrop in the Nørre Lyngby basin (Fig. 6). A 1–2 m high escarpment in the present-day terrain (Fig. 7B) can be interpreted as fault-scarp that runs parallel to the trend of the Børglum fault.

Glacially induced faults have been recognized in Scandinavia for decades now. The Børglum fault closes the gap between the more

recent glacially induced faults observed in southern Sweden (Smith et al., 2014; Jakobsson et al., 2014; Berglund and Dahlström, 2015; Malehmir et al., 2016) and southern Denmark (Sandersen and Jørgensen, 2015) and underlines the observation that these faults are not restricted to areas where the ice sheet reached its maximum thickness. A comparable situation with young tectonic activity between ~15 ka to 13.5 ka is described by Jensen et al. (2002) for the Kattegat area (central portion of the STZ). Jensen et al. (2017) report a neotectonic fault reactivation at the southeastern end of the STZ. Adding the descriptions of deformed Lateglacial and Holocene sediments from the eastern part of the STZ (Gregersen et al., 1996) implies that the entire STZ has been prone to glacially induced faulting.

4.3. Tectonic model

Following Lykke-Andersen (1992) the Nørre Lyngby basin developed as a kind of half-graben related depocenter above a listric normal fault. Based on the field data, digital elevation models and the results from the GIA modelling, a modified tectonic model for the post-glacial activity and related landscape evolution of the northwestern part of the STZ can be developed. The exposure of the Nørre Lyngby basin gives evidence for normal faulting (Figs. 4–6). The numerical simulations show that normal faulting is possible after 18 ka. We note though that a likely explanation for normal faults in such a setting are strike-slip movements along the Børglum fault. New data also indicate a dextral strike-slip nature of the STZ in the Bornholm area (Jensen et al., 2017) and according to Phillips et al. (2017) the STZ represents a long-lived lineament that has been periodically reactivated including both sinistral and dextral movements. This scenario, strike-slip faulting after 18 ka, is also supported by our numerical simulations.

Movements along fault step-overs would result in localized extension and the formation of normal faults as observed in the outcrop. Consequently, the narrow and elongated Nørre Lyngby basin described in Lykke-Andersen (1992) and Fischer et al. (2013) can be alternatively interpreted as a strike-slip basin that developed due to right-lateral movements of the Børglum fault. Lake basins (often termed sag ponds) comparable in geometry are known from active strike-slip faults like the San Andreas Fault (e.g., Sylvester, 1988; Ben-Zion et al., 2012) or the North Anatolian Fault (e.g., Hubert-Ferrari et al., 2002). The basin axis trends E-W and the Børglum fault in this area is interpreted to have a WNW-ESE trend (Figs. 1, 2A and 10A). This obliquity of the basin axis to the Børglum fault implies that the basin formed in a fault step-over situation (Fig. 10B). As shown in Titus et al. (2002), the rhombochasm shape of a pull-apart structure depends on the position of the overlapping faults. A fault overlap, as shown in Fig. 10B, would create a basin that has a comparable geometry as the Nørre Lyngby basin. The trend of the major normal fault in the outcrop (Figs. 6 and 10B) is ENE-WSW (60° to the trend of the Børglum fault), which indicates the related extension that would fit in such a scenario.

Another indicator for strike-slip movements can be found in the local topography. Digital elevation models (Fig. 10A) show narrow and elongated depressions in the area. The work of Keller et al. (1982) shows sag ponds typically associated with strike-slip faults. The topography implies that the potential sag pond in the Løkken area might be related to a fault parallel to the Børglum fault (Fig. 10A). This potentially fault-related depocenter is filled with young Holocene marine deposits (*Littorina* clay; Fig. 3B and C), indicating young fault activity.

In the Løkken area two potential sag ponds merge at a low angle (Fig. 10A). Based on the geometry, these sag ponds resemble the geometry of a fault with a related Riedel shear. Riedel shears are controlled by the angle of internal friction of the host rock (e.g., Bartlett et al., 1981; Katz et al., 2004) and typical intersection angles with the main fault are in a range of 10°–30° (Carne and Little, 2012). The intersection angle of the potential main fault in the Løkken area with the subordinate fault is 25°, which supports a Riedel shear interpretation. The strike-slip interpretation is also supported by the terrain analysis. Plotting the trend of the erosional valleys in a rose diagram (Fig. 7C), shows a pattern that resembles the geometries of a strike-slip fault system with the subordinate Riedel shears and P-shears.

We argue that this is a potential scenario for the fault-related landscape evolution along the Børglum fault, but further investigations (e.g., near-surface geophysical methods such as ground-penetrating radar or shear-wave seismic reflection surveys) are necessary to verify this model. Indubitable is that the Børglum fault was reactivated due to GIA-related stress changes and was prone to strike-slip movements that potentially caused the formation of the elongated Nørre Lyngby lake basin (Fig. 10A). However, it must be kept in mind that the tectonic activity today differs from the activity in the past. Gregersen (1992) already pointed out that there was a strong change in the stress field during the Holocene from a stress field that was dominated by the GIA processes to today's stress field that is controlled by the plate motion. This idea is supported by the results of our numerical simulations. A strike-slip interpretation of the Børglum fault is also supported by modelling results of Kaiser et al. (2005), which show that recent dextral movements at the STZ are still possible in the study area. Today's slip rates are very low as modelled by Kaiser et al. (2005) and the recent seismic activity in this area shows a diffuse pattern (Gregersen et al., 2005). During the Lateglacial, the conditions were different as indicated by fault displacement in a range of 3 m. Large amounts of stress that were stored in the lithosphere over long times, were released due to GIA. This culminated in a phase of strong tectonic activity around ~14.5 to 12 ka as supported by field data and numerical modelling.

We favour a strike-slip model because it connects the outcrop observations and the geomorphology of the area with the numerical simulations of the GIA-related fault reactivation and also takes the dextral strike-slip movements along the STZ into account that were documented in the literature. This result is different compared to our findings for the Osning Thrust in northern Germany (Brandes et al., 2012), where we also relate its reactivation to GIA but in a thrust-fault regime, and where we could exclude normal and strike-slip faulting. We attribute this to the fact that the Osning Thrust is in the peripheral bulge area of the former ice sheet further south of the STZ and is more likely susceptible to thrust faulting due to its orientation within the plate motion-induced stress field.

North and south of the Nørre Lyngby basin small-scale depocenters occur that are filled with either marine or terrestrial sediments (Jessen and Nordmann, 1915; Lykke-Andersen, 1992; Sadolin et al., 1997; Richardt, 1998; Pedersen, 2005; Fischer et al., 2013). The formation of these depocenters is not well constrained but it is possible that some of these mini-basins have a comparable, fault-controlled origin as the Nørre Lyngby basin and therefore also can be related to the proposed strike-slip tectonics within this part of the STZ. Evidence is given by shape of the basins, sediment deformations, faulting and the down-warping of the underlying older marine sediments.

5. Conclusions

Normal faults and soft-sediment deformation structures developed in Lateglacial shallow marine and lake deposits around the Sorgenfrei-Tornquist Zone provide evidence for neotectonic activity along the Børglum fault that was accompanied by seismic

activity at around 14.5 to 12 ka. These geological features as well as the formation of local Lateglacial mini-basins can be explained with a strike-slip model that originates from the dominant plate motion-induced stress pattern (NW-SE) in northern and central Europe. The timing of the deformation and numerical simulations of the deglaciation-related lithospheric stress build-up indicate that these tectonic movements were most likely controlled by stress changes, which were induced by the decay of the Scandinavian ice sheet. Therefore, this part of the Sorgenfrei-Tornquist Zone can be interpreted as susceptible to glacially induced faulting, which closes the gap between the more recent glacially induced faults observed in southern Sweden (Smith et al., 2014; Jakobsson et al., 2014; Berglund and Dahlström, 2015; Malehmir et al., 2016) and southern Denmark (Sandersen and Jørgensen, 2015). Data from other studies imply that glacially induced faulting probably applies to the entire Sorgenfrei-Tornquist Zone.

Acknowledgements

The ANU-ICE models were kindly provided by Kurt Lambeck and Anthony Purcell. We are grateful to Jonathan Lee for the constructive review that helped to improve the manuscript. Many thanks to David Tanner for discussion.

Appendix A. Supplementary data

Supplementary data related to this article can be found at https://doi.org/10.1016/j.quascirev.2018.03.036.

References

Alfaro, P., Delgado, J., Estévez, A., Molina, J.M., Moretti, M., Soria, J.M., 2002. Liquefaction and fluidization structures in Messinian storm deposits (Bajo Segura Basin, Betic Cordillera, southern Spain). Int. J. Earth Sci. 91 (3), 505–513.
Al Hseinat, M., Hübscher, C., 2014. Ice-load induced tectonics controlled tunnel valley evolution - instances from the southwestern Baltic Sea. Quat. Sci. Rev. 97, 121–135.
Al Hseinat, M., Hübscher, C., 2017. Late Cretaceous to recent tectonic evolution of the north German Basin and the transition zone to the Baltic shield/southwest Baltic Sea. Tectonophysics 708, 28–55.
Anand, A., Jain, A.K., 1987. Earthquakes and deformational structures (seismites) in Holocene sediments from the Himalayan-Andaman Arc, India. Tectonophysics 133, 105–120.
Argus, D.F., Peltier, W., Drummond, R., Moore, A.W., 2014. The Antarctica component of postglacial rebound model ICE-6G_C (VM5a) based on GPS positioning, exposure age dating of ice thicknesses, and relative sea level histories. Geophys. J. Int. 198 (1), 537–563.
Arvidsson, R., 1996. Fennoscandian earthquakes: whole crustal rupturing related to postglacial rebound. Science 274, 744–746.
Bartlett, W.L., Friedman, M., Logan, J.M., 1981. Experimental folding and faulting of rocks under confining pressure. Tectonophysics 79, 255–277.
Bayer, U., Scheck, M., Rabbel, W., Krawczyk, C.M., Götze, H.-J., Stiller, M., Beilecke, T., Marotta, A.M., Barrio-Alvers, L., Kuder, J., 1999. An integrated study of the NE German Basin. Tectonophysics 314, 285–307.
Ben-Zion, Y., Rockwell, T.K., Shi, Z., Xu, S., 2012. Reversed-polarity secondary deformation structures near fault stepovers. J. Appl. Mech. 79, 031025.
Berglund, M., Dahlström, N., 2015. Post-glacial fault scarps in Jämtland, central Sweden. GFF 137, 339–343.
Berra, F., Felletti, F., 2011. Syndepositional tectonics recorded by soft-sediment deformation and liquefaction structures (continental Lower Permian sediments, Southern Alps, Northern Italy): stratigraphic significance. Sediment. Geol. 235, 249–263.
Berthelsen, A., 1998. The Tornquist Zone northwest of the Carpathians: an intraplate pseudosuture. GFF 120, 223–230.
Binzer, K., Stockmarr, J., 1994. Geologisk kort over Danmark. Prækvartæroverf ladens højdeforhold. Danmarks Geologiske Undersøgelse Kortserie 44, 10 pp. (In Danish).
Böse, M., Lüthgens, C., Lee, J.R., Rose, J., 2012. Quaternary glaciations of northern Europe. Quat. Sci. Rev. 44, 1–25.
Brandes, C., Tanner, D.C., 2012. Three-dimensional geometry and fabric of shear deformation-bands in unconsolidated Pleistocene sediments. Tectonophysics 518–521, 84–92.
Brandes, C., Winsemann, J., 2013. Soft-sediment deformation structures in NW Germany caused by Late Pleistocene seismicity. Int. J. Earth Sci. 102, 2255–2274.
Brandes, C., Winsemann, J., Roskosch, J., Meinsen, J., Tanner, D.C., Frechen, M., Steffen, H., Wu, P., 2012. Activity of the Osning thrust in Central Europe during the Late glacial: ice-sheet and lithosphere interactions. Quat. Sci. Rev. 38, 49–62.
Brandes, C., Schmidt, C., Tanner, D.C., Winsemann, J., 2013. Paleostress pattern and salt tectonics within a developing foreland basin (north-western Subhercynian Basin, northern Germany). Int. J. Earth Sci. 102, 2239–2254.
Brandes, C., Steffen, H., Steffen, R., Wu, P., 2015. Intraplate seismicity in northern Central Europe is induced by the last glaciation. Geology 43, 611–614.
Brandes, C., Igel, J., Loewer, M., Tanner, D.C., Lang, J., Müller, K., Winsemann, J., 2018. Visualisation and analysis of shear-deformation bands in unconsolidated Pleistocene sand using ground-penetrating radar: implications for paleoseismological studies. Sediment. Geol. 367, 135–145.
Britze, P., Japsen, P., 1991. Geological Map of Denmark 1:400 000: the Danish Basin: «Top Zechstein» and the Triassic (Two-way Travel Time and Depth, Thickness and Interval Velocity). Geological Survey of Denmark, pp. 1–4. Map Series No. 31, ISSN : 0901-9405.
Carne, R.C., Little, T.A., 2012. Geometry and scale of fault segmentation and deformational bulging along an active oblique-slip fault (Wairarapa fault, New Zealand). GSA Bulletin 124, 1365–1381.
Chen, J., Lee, H.S., 2013. Soft-sediment deformation structures in Cambrian siliciclastic and carbonate storm deposits (Shandong Province, China): differential liquefaction and fluidization triggered by storm-wave loading. Sediment. Geol. 288, 81–94.
Cotte, N., Pedersen, H.A., TOR Working Group, 2002. Sharp contrast in lithospheric structure across the Sorgenfei-Tornquist Zone as inferred by Rayleigh wave analysis of TOR1 project data. Tectonophysics 360, 75–88.
Davison, C., 1921. A Manual of Seismology. The University Press, 256 pp.
Dehls, J.F., Olesen, O., Olsen, L., Blikra, L.H., 2000. Neotectonic faulting in northern Norway; the Stuoragurra and Nordmannvikdalen postglacial faults. Quat. Sci. Rev. 19, 1447–1460.
Erlström, M., Thomas, S.A., Deeks, N., Sivhed, U., 1997. Structure and tectonic evolution of the Tornquist Zone and adjacent sedimentary basins in Scania and the southern Baltic Sea area. Tectonophysics 271, 191–215.
Fischer, A., Clemmensen, L.B., Donahue, R., Heinemeier, J., Lykke-Andersen, H., Lysdahl, P., Mortensen, M.F., Olsen, J., Petersen, P.V., 2013. Late Paleolithic Nørre Lyngby – a northern outpost close to the west coast of Europe. Quartar 60, 137–162.
Fossen, H., Schultz, R.A., Shipton, Z.K., Mair, K., 2007. Deformation bands in sandstone: a review. J. Geol. Soc. 164, 755–769.
French, H.M., 2007. The Periglacial Environment, third ed. Wiley. 478 pp.
Galli, P., 2000. New empirical relationships between magnitude and distance for liquefaction. Tectonophysics 324, 169–187.
Grand, S.P., Van Der Hilst, R.D., Widiyantoro, S., 1997. Global seismic tomography: a snapshot of convection in the Earth. Geol. Soc. Am. 7 (4), 1–7.
Gregersen, S., 1992. Crustal stress regime in Fennoscandia from focal mechanisms. J. Geophys. Res. 97, 11821–11827.
Gregersen, S., 2002. Earthquakes and change of stress since the ice age in Scandinavia. Bull. Geol. Soc. Den. 49, 73–78.
Gregersen, S., Voss, P., 2009. Stress change over short geological time: the case of Scandinavia over 9000 years since the Ice Age. In: Reicherter, K., Michetti, A.M., Silva Barroso, P.G. (Eds.), Palaeoseismology: Historical and Prehistorical Records of Earthquake Ground Effects for Seismic Hazard Assessment. Geological Society of London, Special Publications 316, pp. 173–178.
Gregersen, S., Voss, P.H., 2012. Efforts to include geological and geodetic observations in the assessment of earthquake activity in Denmark. Geol. Surv. Den. Greenl. Bull. 26, 41–44.
Gregersen, S., Voss, P.H., 2014. Review of some significant claimed irregularities in Scandinavian postglacial uplift on timescales of tens of thousands of years – earthquakes in Denmark? Solid Earth 5, 109–118.
Gregersen, S., Leth, J., Lind, G., Lykke-Andersen, H., 1996. Earthquake activity and its relationship with geologically recent motion in Denmark. Tectonophysics 257, 265–273.
Gregersen, S., Glendrup, M., Larsen, T.B., Voss, P., Rasmussen, H.P., 2005. Seismology: neotectonics and structure of the Baltic shield. Geol. Surv. Den. Greenl. Bull. 7, 25–28.
Grollimund, B., Zoback, M.D., 2001. Did deglaciation trigger intraplate seismicity in the New Madrid seismic zone? Geology 29, 175–178.
Guiter, F., Andrieu-Ponel, V., de Beaulieu, J.-L., Cheddadi, R., Calvez, M., Ponel, P., Reille, M., Keller, T., Goeury, C., 2003. The last climatic cycles in Western Europe: a comparison between long continuous lacustrine sequences from France and other terrestrial records. Quat. Int. 111, 59–74.
Hampel, A., 2017. Response of faults to climate-induced changes of ice-sheets, glaciers and lakes. Geol. Today 33 (1), 12–18.
Hampel, A., Hetzel, R., 2006. Response of normal faults to glacial-interglacial fluctuations of ice and water masses on Earth's surface. J. Geophys. Res. 111, B06406. https://doi.org/10.1029/2005JB004124.
Hampel, A., Hetzel, R., Maniatis, G., Karow, T., 2009. Three-dimensional numerical modeling of slip rate variations on normal and thrust fault arrays during ice cap growth and melting. J. Geophys. Res. 114, B08406. https://doi.org/10.1029/2008JB006113.
Hampel, A., Karow, T., Maniatis, G., Hetzel, R., 2010. Slip rate variations on faults during glacial loading and postglacial unloading: implications for the viscosity structure of the lithosphere. In: C. Pascal, I.S. Stewart, B.L.A. Vermeersen, Neotectonics, Seismicity and Stress in Glaciated Regions. J. Geol. Soc. Lond. 167, 385–399.

Hansen, D.L., Nielsen, S.B., Lykke-Andersen, H., 2000. The post-Triassic evolution of the Sorgenfei-Tornquist Zone – results from thermo-mechanical modelling. Tectonophysics 328, 245–267.
Hatcher Jr., R.D., Vaughn, J.D., Obermeier, S.F., 2012. Large earthquake paleoseismology in the East Tennessee seismic zone: results of an 18-month pilot study. In: Cox, R.T., Tuttle, M.P., Boyd, O.S., Locat, J. (Eds.), Recent Advances in North American Paleoseismology and Neotectonics East of the Rockies: Geological Society of America Special Paper 493, pp. 111–142.
Hetzel, R., Hampel, A., 2005. Slip rate variations on normal faults during glacial-interglacial changes in surface loads. Nature 435, 81–84.
Hillis, R.R., Holford, S.P., Green, P.F., Doré, A.G., Gatliff, R.W., Stoker, M.S., Thomson, K., Turner, J.P., Underhill, J.R., Williams, G.A., 2008. Cenozoic exhumation of the southern British Isles. Geology 36, 371–374.
Hoffmann, G., Reicherter, K., 2012. Soft-sediment deformation of late Pleistocene sediments along the southwestern coast of the Baltic Sea (NE Germany). Int. J. Earth Sci. 101, 351–363.
Holford, S.P., Turner, J.P., Green, P.F., 2005. Reconstructing the Mesozoic–Cenozoic exhumation history of the Irish Sea basin system using apatite fission track analysis and vitrinite reflectance data. In: Doré, A.G., Vining, B.A. (Eds.), Petroleum Geology: North-West Europe and Global Perspectives – Proceedings of the 6th Peroleum Geology Conference. Geological Society, London, pp. 1095–1107.
Holford, S.P., Green, P.F., Duddy, I.R., Turner, J.P., Hillis, R.R., Stoker, M.S., 2009. Regional intraplate exhumation episodes related to plate-boundary deformation. Geol. Soc. Am. Bull. 121, 1611–1628.
Houmark-Nielsen, M., 2007. Extent and age of Middle and Late Pleistocene glaciations and periglacial episodes in southern Jylland, Denmark. Bull. Geol. Soc. Den. 55, 9–35.
Houmark-Nielsen, M., Kjær, K.H., 2003. Southwest Scandinavia, 40–15 kyr BP: palaeogeography and environmental change. J. Quat. Sci. 18, 769–786.
Hubert-Ferrari, A., Armijo, R., King, G., Meyer, B., Barka, A., 2002. Morphology, displacement, and slip rates along the north Anatolian Fault, Turkey. J. Geophys. Res. 107 (No. B10), 2235. https://doi.org/10.1029/2001JB000393.
Hughes, A.L.C., Gyllencreutz, R., Lohne, Ø.S., Mangerud, J., Svendsen, J.I., 2016. The last Eurasian ice sheets – a chronoloical database and time-slice reconstruction, DATED-1. Boreas 45, 1–45.
Huuse, M., Lykke-Andersen, H., Michelsen, O., 2001. Cenozoic evolution of the eastern Danish North Sea. Mar. Geol. 177, 243–269.
Iversen, J., 1973. The Development of Denmark's Nature Since the Last Glacial. C.A. Reitzel, Copenhagen. V. Series, No. 7-C, 126 pp.
Jakobsson, M., Björck, S., O'Regan, M., Flodén, T., Greenwood, S.L., Swärd, H., Lif, A., Ampel, L., Koyi, H., Skelton, A., 2014. Major earthquake at the Pleistocene-Holocene transition in Lake Vättern, southern Sweden. Geology 42, 379–382.
Japsen, P., Bidstrup, T., 1999. Quantification of late Cenozoic erosion in Denmark based on sonic data and basin modelling. Bull. Geol. Soc. Den. 46, 79–99.
Japsen, P., Langtofte, C., 1991. Geological map of Denmark, 1:400.000. Geological Survey of Denmark, Copenhagen. Map Series No. 29, 8 pp.
Jensen, J.B., Petersen, K.S., Konradi, P., Kuijpers, A., Bennike, O., Lemke, W., Endler, R., 2002. Neotectonics, sea-level changes and biological evolution in the fenno-scandian Border zone of the southern Kattegat sea. Boreas 31, 133–150.
Jensen, J.B., Moros, M., Endler, R., IODP Expedition 347 Members, 2017. The Bornholm Basin, southern Scandinavia: a complex history from Late Cretaceous structural developments to recent sedimentation. Boreas 46, 3–17.
Jessen, A., 1918. Vendsyssels Geologi. Danmarks Geologiske Undersøgelse. V Række 2, 260 pp. (In Danish).
Jessen, A., 1931. Lønstrup Klint. Danmarks Geologiske Undersøgelse, 142 pp. (In Danish).
Jessen, A., 1936. Vendsyssels geologi (the geology of Vendsyssel). Geol. Surv. Den. Greenl. V. (No. 2), 195 pp. (In Danish).
Jessen, A., Nordmann, V., 1915. Ferskvandslagene ved Nørre Lyngby. Summary: the Fresh-water Deposits at Nørre Lyngby. Geological Survey of Denmark, Reitzel, Copenhagen. II Series, no. 29, 66 pp, (In Danish).
Johnston, P., Lambeck, K., 1999. Postglacial rebound and sea level contributions to changes in the geoid and the Earth's rotation axis. Geophys. J. Int. 136, 537–558.
Kaiser, A., Reicherter, K., Hübscher, C., Gajewski, D., 2005. Variation of the present-day stress field within the North German Basin – insights from thin shell FE modeling based on residual GPS velocities. Tectonophysics 397, 55–72.
Kasse, C., Vandenberghe, D., De Corta, F., Van den Haute, P., 2007. Late Weichselian fluvio-aeolian sands and coversands of the type locality Grubbenvorst (southern Netherlands): sedimentary environments, climate record and age. J. Quat. Sci. 22, 695–708.
Katz, Y., Weinberger, R., Aydin, A., 2004. Geometry and kinematic evolution of Riedel shear structures, Capitol Reef National Park, Utah. J. Struct. Geol. 26, 491–501.
Kaufmann, G., Wu, P., 2002. Glacial isostatic adjustment in Fennoscandia with a three-dimensional viscosity structure as an inverse problem. Earth Planet Sci. Lett. 197, 1–10.
Kaufmann, G., Wu, P., Li, G., 2002. Glacial isostatic adjustment in Fennoscandia for a laterally heterogeneous earth. Geophys. J. Int. 143, 262–273.
Keller, E.A., Bonkowski, M.S., Korsch, R.J., Shlemon, R.J., 1982. Tectonic geomorphology of the san Andreas Fault zone in the southern Indio Hills, Coachella Valley, California. GSA Bulletin 93, 46–56.
Kierulf, H.P., Steffen, H., Simpson, M.J.R., Lidberg, M., Wu, P., Wang, H., 2014. A GPS velocity field for Fennoscandia and a consistent comparison to glacial isostatic adjustment models. J. Geophys. Res.: Solid Earth 119 (8), 6613–6629.
Kley, J., Voigt, T., 2008. Late Cretaceous intraplate thrusting in central Europe: effect of Africa-Iberia-Europe convergence, not Alpine collision. Geology 36, 839–842.
Knudsen, K.L., 1978. Middle and Late Weichselian Marine Deposits at Nørre Lyngby, Northern Jutland, Denmark, and Their Foraminiferal Faunas. Geological Survey of Denmark. II.Series, No. 112, 44 pp.
Krawczyk, C.M., McCann, T., Cocks, L.R.M., England, R.W., McBride, J.H., Wybraniec, S., 2008. Caledonian tectonics. In: McCann, T. (Ed.), The Geology of Central Europe. Precambrian and Paleozoic, vol. 1. Geological Society, London, pp. 303–381.
Kristensen, M.B., Childs, C., Olesen, N.Ø., Korstgård, J.A., 2013. The microstructure and internal architecture of shear bands in sand-clay sequences. J. Struct. Geol. 46, 129–141.
Krog, H., 1978. The Late Weichselian freshwater bed at Nørre Lyngby. C-14 dates and pollen diagram. Danm. Geol. Unders. DGU Åborg 1976, 29–43.
Krohn, C.F., Larsen, N.K., Kronborg, C., Nielsen, O.B., Knudsen, K.L., 2009. Litho-and chronostratigraphy of the Late Weichselian in Vendsyssel, northern Denmark, with special emphasis on tunnel-valley infill in relation to a receding ice margin. Boreas 38, 811–833.
Kujansuu, R., 1964. Nuorista siirroksista Lapissa. Summary: recent faults in Lapland. Geologi, Vsk 16, 30–36 (In Finnish).
Kukkonen, I.T., Olesen, O., Ask, M.V.S., PFDP Working Group, 2010. Postglacial faults in Fennoscandia: targets for scientific drilling. GFF 132 (1), 71–81.
Lagerbäck, R., 1978. Neotectonic structures in northern Sweden. GFF (Geol. Foren. Stockh. Forh.) 100, 263–269.
Lagerbäck, R., Sundh, M., 2008. Early Holocene Faulting and Paleoseismicity in Northern Sweden. SGU Research paper C386.
Lambeck, K., 1995. Late devensian and Holocene shorelines of the British Isles and north sea from models of glacio-hydro-isostatic rebound. J. Geol. Soc. Lond 152, 437–448.
Lambeck, K., Purcell, A., Zhao, J., Svensson, N.-O., 2010. The Scandinavian ice sheet: from MIS 4 to the end of the last glacial maximum. Boreas 39 (2), 410–435.
Lang, J., Böhner, U., Polom, U., Serangeli, J., Winsemann, J., 2015. The middle Pleistocene tunnel valley at Schöningen as a paleolithic archive. J. Hum. Evol. 89, 18–26.
Larsen, N.K., Knudsen, K.L., Krohn, C.F., Kronborg, C., Murray, A.S., Nielsen, O.B., 2009. Late Quaternary ice sheet, lake and sea history of southwest Scandinavia–a synthesis. Boreas 38, 732–761.
Lee, J.R., Wakefield, O.J.W., Phillips, E., Hughes, L., 2015. Sedimentary and structural evolution of a relict subglacial to subaerial drainage system and its hydro-geological implications: an example from Anglesey, north Wales, UK. Quat. Sci. Rev. 109, 88–110.
Lindblom, E., Lund, B., Tryggvason, A., Uski, M., Bödvarsson, R., Juhlin, C., Roberts, R., 2015. Microearthquakes illuminate the deep structure of the endglacial Pärvie fault, northern Sweden. Geophys. J. Int. 201, 1704–1716.
Lowe, D.R., 1975. Water escape structures in coarse-grained sediments. Sedimentology 22, 157–204.
Lund, B., 2015. Palaeoseismology of glaciated terrain. In: Beer, M., et al. (Eds.), Encyclopedia of Earthquake Engineering. Springer-Verlag, Berlin, Heidelberg, pp. 1765–1779. https://doi.org/10.1007/978-3-642-36197-5_25-1.
Lund, B., Schmidt, P., Hieronymus, C., 2009. Stress Evolution and Fault Stability during the Weichselian Glacial Cycle. SKB Technical report no TR-09–15. Swedish Nuclear Fuel and Waste Management Co. (SKB), Stockholm.
Lykke-Andersen, H., 1979. Nogle undergrundstektoniske elementer i det danske Kvataer. Dansk geol. Foren 1–7 (In Danish).
Lykke-Andersen, H., 1992. Massebevægelser i Vendsyssels og Kattegats kvartære aflejringer. Dansk. Geol. Foren. Årsskrift for 1990–91, 93–97 (In Danish).
Lykke-Andersen, H., Borre, K., 2000. Aktiv tektonik i Danmark – der er liv i Sorgenfrei-Tornquist Zonen. Geologisk Nyt 6/00, 12–13 (In Danish).
Malehmir, A., Andersson, M., Mehta, S., Brodic, B., Munier, R., Place, J., Maries, G., Smith, C., Kamm, J., Bastani, M., Mikko, H., Lund, B., 2016. Post-glacial reactivation of the Bollnäs fault, central Sweden - a multidisciplinary geophysical investigation. Solid Earth 7, 509–527.
Mazur, S., Mikolajczak, M., Krzywiec, P., Malinowski, M., Buffenmyer, V., Lewandowski, M., 2015. Is the Teisseyre-Tornquist zone an ancient plate boundary of Baltica? Tectonics 34, 2465–2477.
Mazur, S., Mikolajczak, M., Krzywiec, P., Malinowski, M., Buffenmyer, V., Lewandowski, M., 2016. Reply to comment by M. Narkiewicz and Z. Petecki on "is the Teisseyre-Tornquist zone an ancient plate boundary of Baltica?". Tectonics 35, 1600–1607.
Meier, D., Kronberg, P., 1989. Klüftung in Sedimentgestein. Enke Verlag Stuttgart 116 pp. (In German).
Meinsen, J., Winsemann, J., Roskosch, J., Brandes, C., Frechen, M., Böttcher, J., Dultz, S., 2014. Climate control on the evolution of Late Pleistocene alluvial fan and aeolian sand-sheet systems in NW Germany. Boreas 43, 42–66.
Michelsen, O., 1997. Mesozoic and Cenozoic stratigraphy and structural development of the Sorgenfrei-Tornquist zone. ZDGG 148, 33–50.
Michelsen, O., Nielsen, L.H., 1991. Well records on the phanerozoic stratigraphy in the fennoscandian Border zone, Denmark. Hans-1, Sæby-1, and Terne-1 wells. Geol. Surv. Den. Series A 29, 39 pp.
Michelsen, O., Nielsen, L.H., 1993. Structural development of the fennoscandian Border zone, offshore Denmark. Mar. Petrol. Geol. 10, 124–134.
Mikko, H., Smith, C.A., Lund, B., Ask, M.V.S., Munier, R., 2015. LiDAR-derived inventory of post-glacial fault scarps in Sweden. GFF 137, 334–338.
Mogensen, T.E., 1994. Palaeozoic structural development along the Tornquist zone, Kattegat area, Denmark. Tectonophysics 240, 191–214.

Mogensen, T.E., Korstgård, J.A., 2003. Triassic and Jurassic transtension along part of the Sorgenfrei-Tornquist zone in the Danish Kattegat. Geol. Surv. Den. Greenl. Bull. 1, 439–458.
Mörner, N.-A., 1978. Faulting, fracturing, and seismicity as functions of glacio-isostasy in Fennoscandia. Geology 6, 41–45.
Mörner, N.-A., 2011. Paleoseismology: the application of multiple parameters in four case studies in Sweden. Quat. Int. 242, 65–75.
Narkiewicz, M., Petecki, Z., 2016. Comment on "Is the Teisseyre-Tornquist Zone an ancient plate boundary of Baltica?" by Mazur et al. Tectonics 35, 1595–1599.
Nielsen, S.B., Stephenson, R., Schiffer, C., 2014. Deep controls on intraplate basin inversion. In: Talwani, P. (Ed.), Intraplate Earthquakes, pp. 257–274.
Ojala, V.J., Kuivamäki, A., Vuorela, P., 2004. Postglacial deformation of bedrock in Finland. Geol. Surv. Finland. Nuclear Waste Disposal Research, Report YST-120, 23 pp.
Ojala, A.E.K., Mattila, J., Ruskeeniemi, T., Palmu, J.-P., Lindberg, A., Hänninen, P., Sutinen, R., 2017. Postglacial seismic activity along the Isovaara–Riikonkumpu fault complex. Global Planet. Change 157, 59–72.
Owen, G., 1996. Experimental soft-sediment deformation: structures formed by the liquefaction of unconsolidated sands and some ancient examples. Sedimentology 43, 279–293.
Owen, G., Moretti, M., 2011. Identifying triggers for liquefaction-induced soft-sediment deformation in sands. Sediment. Geol. 235, 141–147.
Palmu, J.-P., Ojala, A.E.K., Ruskeeniemi, T., Sutinen, R., Mattila, J., 2015. LiDAR DEM detection and classification of postglacial faults and seismically-induced landforms in Finland: a paleoseismic database. GFF 137, 344–352.
Papadopoulos, G.A., Lefkopoulos, G., 1993. Magnitude-Distance relations for liquefaction in soil from earthquakes. Bull Seis Soc Am 83, 925–938.
Pedersen, S.A.S., 2005. Structural analysis of the Rubjerg Knude glaciotectonic complex, Vendsyssel, northern Denmark. Geol. Surv. Den. Greenl. Bull. 8, 1–192.
Pedersen, S.A.S., Gravesen, P., 2010. Low- and Intermediate Level Radioactive Waste from Risø, Denmark. Location Studies for Potential Disposal Areas. Report No. 3: Geological Setting and Tectonic Framework in Denmark. Geological Survey of Denmark and Greenland Report 2010/124, 51 pp..
Pedersen, S.A.S., Hermansen, B., Nathan, C., Tougaard, L., 2011. Digitalt kort over Danmarks jordarter 1:200.000 (Digital soil map of Denmark), Version 2. Geologisk kort over de overfladenære jordarter i Danmark. Geological Survey of Denmark and Greenland, Report 2011/19, 9 pp. (In Danish).
Pedersen, T., Gregersen, S., TOR working group, 1999. Project Tor: Deep lithospheric variation across the Sorgenfrei-Tornquist Zone, Southern Scandinavia. Bull. Geol. Soc. Den. 46, 13–24.
Peltier, W., Argus, D., Drummond, R., 2015. Space geodesy constrains ice age terminal deglaciation: the global ICE-6G_C (VM5a) model. J. Geophys. Res.: Solid Earth 120 (1), 450–487.
Penney, D.N., 1985. The Holocene marine sequence in the Løkken area of Vendsyssel, Denmark. Eiszeitalt. Ggw. 35, 79–88.
Phillips, E., Hughes, L., 2014. Hydrofracturing in response to the development of an overpressurised subglacial meltwater system during drumlin formation: an example from Anglesey, NW Wales. Proc. Geologists' Assoc. 125, 296–311.
Phillips, E., Everest, J., Reeves, H., 2013. Micromorphological evidence for subglacial multiphase sedimentation and deformation during overpressurized fluid flow associated with hydrofracturing. Boreas 42, 395–427.
Phillips, T.B., Jackson, C.A.-L., Bell, R.E., Duffy, O.B., 2017. Oblique reactivation of lithosphere-scale lineaments controls rift physiography – the upper crustal expression of the Sorgenfrei-Tornquist Zone, offshore southern Norway. Solid Earth Discuss. https://doi.org/10.5194/se-2017-97 7 September 2017.
Rasmussen, E.S., 2009. Neogene inversion of the central graben and Ringkøbing-fyn High, Denmark. Tectonophysics 465, 84–97.
Richardt, N., 1996. Sedimentological examination of the Late Weichselian sea-level history following deglaciation of northern Denmark. In: Andrews, J.T., Austin, W.E.N., Bergsten, H., Jennings, A.E. (Eds.), Late Quaternary Palaeoceanography of the North Atlantic Margins Geological Society. Special Publications 111, London, pp. 261–273.
Richardt, N., 1998. Marine Sedimentary Environments, Sea-level History, and Deglaciation; Late Weichselian Vendsyssel. University of Copenhagen, Denmark, p. 99. PhD thesis.
Ringrose, P.S., 1989. Palaeoseismic (?) liquefaction event in late Quaternary lake sediment at Glen Roy, Scotland. Terra. Nova 1, 57–62.
Rodríguez-Pascua, M.A., Calvo, J.P., De Vicente, G., Gómez-Gras, D., 2000. Soft-sediment deformation structures interpreted as seismites in lacustrine sediments of the Prebetic Zone, SE Spain, and their potential use as indicators of earthquake magnitudes during the Late Miocene. Sediment. Geol. 135, 117–135.
Rossetti, D.F., 1999. Soft-sediment deformation structures in late Albian to Cenomanian deposits, São Luís Basin, northern Brazil: evidence for palaeoseismicity. Sedimentology 46, 1065–1081.
Root, B.C., van der Wal, W., Novak, P., Ebbing, J., Vermeersen, L.L.A., 2015. Glacial isostatic adjustment in the static gravity field of Fennoscandia. J. Geophys. Res.: Solid Earth 120 (1), 503–518.
Sadolin, M., Pedersen, G.K., Pedersen, S.A.S., 1997. Lacustrine sedimentation and tectonics: an example from the Weichselian at Lønstrup Klint, Denmark. Boreas 26, 113–126.
Sandersen, P., Jørgensen, F., 2002. Kortlægning Af Begravede Dale I Jylland Og På Fyn (Mapping of Buried Valleys in Jutland and Funen). pdatering 2001-2002 (Update 2001-2002). De jysk-fynske amters grundvandssamarbejde Vejle Amt, WaterTech a/s, 189 pp. (In Danish).
Sandersen, P.B.E., Jørgensen, F., 2015. Neotectonic deformation of a Late Weichselian outwash plain by deglaciation-induced fault reactivation of a deep-seated graben structure. Boreas 44, 413–431.
Sandersen, P.B.E., Jørgensen, F., 2016. Kortlægning Af Begravede Dale I Danmark (Mapping of Buried Valleys in Denmark). Opdatering 2015 (Update 2015). GEUS Special Publication, December 2016, Volumes 1 & 2 (In Danish). ISBN: 978-87-7871-451-0/978-87-7871-452-7.
Scheck, M., Bayer, U., Otto, V., Lamarche, J., Banka, D., Pharaoh, T., 2002. The Elbe fault system in north central Europe—a basement controlled zone of crustal weakness. Tectonophysics 360, 281–299.
Seilacher, A., 1969. Fault-graded beds interpreted as seismites. Sedimentology 13, 155–159.
Selsing, L., 1981. Stress analysis on conjugate normal faults in unconsolidated Weichselian glacial sediments from Brorfelde, Denmark. Boreas 10, 275–279.
Smit, J., van Wees, J.-D., Cloetingh, S., 2016. The Thor suture zone: from subduction to intraplate basin setting. Geology 44, 707–710.
Smith, C.A., Sundh, M., Mikko, H., 2014. Surficial geology indicates early Holocene faulting and seismicity, central Sweden. Int. J. Earth Sci. 103, 1711–1724.
Steffen, H., Kaufmann, G., Wu, P., 2006. Three-dimensional finite-element modelling of the glacial isostatic adjustment in Fennoscandia. Earth Planet Sci. Lett. 250, 358–375.
Steffen, R., Wu, P., Steffen, H., Eaton, D.W., 2014a. On the implementation of faults in finite-element glacial isostatic adjustment models. Comput. Geosci. 62, 150–159.
Steffen, R., Wu, P., Steffen, H., Eaton, D.W., 2014b. The effect of earth rheology and ice-sheet size on fault-slip and magnitude of postglacial earthquakes. Earth Planet Sci. Lett. 388, 71–80.
Steffen, R., Steffen, H., Wu, P., Eaton, D.W., 2014c. Stress and fault parameters affecting fault slip magnitude and activation time during a glacial cycle. Tectonics 33, 1461–1476.
Stein, S., Cloetingh, S., Sleep, N.H., Wortel, R., 1989. Passive Margin earthquakes, stresses and rheology. In: Gregersen, S., Basham, P.W. (Eds.), Earthquakes at North Atlantic Passive Margins: Neotectonics and Postglacial Rebound. Kluwer, Dordrecht, pp. 231–259.
Stewart, I.S., Sauber, J., Rose, J., 2000. Glacio-seismotectonics: ice sheets, crustal deformation and seismicity. Quat. Sci. Rev. 19, 1367–1389.
Sutinen, R., Hyvönen, E., Middleton, M., Ruskeeniemi, T., 2014. Airborne LiDAR detection of postglacial faults and pulju moraine in palojärvi, Finnish Lapland. Global Planet. Change 115, 24–32.
Sylvester, A.G., 1988. Strike-slip faults. GSA Bulletin 100, 1666–1703.
Tanner, B., Meissner, R., 1996. Caledonian deformation upon southwest Baltica and its tectonic implications: alternatives and consequences. Tectonics 15, 803–812.
Ter-Borch, N., 1991. Geological Map of Denmark, 1:500.000. Structural Map of the Top Chalk Group. Geological Survey of Denmark, Copenhagen. Map Series No. 7, 4 pp.
Titus, S.J., Fossen, H., Pedersen, R.B., Vigneresse, J.L., Tikoff, B., 2002. Pull-apart formation and strike-slip partitioning in an obliquely divergent setting, Leka Ophiolite, Norway. Tectonophysics 354, 101–119.
Thybo, H., 1997. Geophysical characteristics of the Tornquist Fan area, northwest Trans-European Suture Zone: indication of late Carboniferous to early Permian dextral transtension. Geol. Mag. 134, 597–606.
Thybo, H., 2000. Crustal structure and tectonic evolution of the Tornquist Fan region as revealed by geophysical methods. Bull. Geol. Soc. Den. 46, 145–160.
Torsvik, T.H., Rehnström, E.F., 2003. The Tornquist Sea and Baltica – Avalonia docking. Tectonophysics 362, 67–82.
Turner, F., Tolksdorf, J.F., Viehberg, F., Schwalb, A., Kaiser, K., Bittmann, F., von Bramann, U., Pott, R., Staesche, U., Breest, K., Veil, S., 2013. Lateglacial/early Holocene fluvial reactions of the Jeetzel river (Elbe valley, northern Germany) to abrupt climatic and environmental changes. Quat. Sci. Rev. 60, 91–109.
Turpeinen, H., Hampel, A., Karow, T., Maniatis, G., 2008. Effect of ice sheet growth and melting on the slip evolution of thrust faults. Earth Planet Sci. Lett. 269, 230–241.
Vandenberghe, J., 2008. The fluvial cycle at cold-warm-cold transitions in lowland regions: a refinement of theory. Geomorphology 98, 275–284.
van Loon, A.J., 2009. Soft-sediment deformation structures in siliciclastic sediments: an overview. Geologos 15, 3–55.
van Loon, A.J., Pisarska-Jamrozy, M., 2014. Sedimentological evidence of Pleistocene earthquakes in NW Poland induced by glacio-isostatic rebound. Sediment. Geol. 300, 1–10.
van Loon, A.J., Pisarska-Jamroży, M., Nartišs, M., Krievāns, M., Soms, J., 2016. Seismites resulting from high-frequency, high-magnitude earthquakes in Latvia caused by Late Glacial glacio-isostatic uplift. J. Palaeogeogr. 5, 363–380.
Vejbæk, O.V., Britze, P., 1994. Geological map of Denmark, 1:750.000. Top Pre-Zechstein (two-way traveltime and depth). GeologicalSurvey of Denmark, Copenhagen. Map Series No. 45, 8 pp.
Wang, H., Wu, P., 2006. Effects of lateral variations in lithospheric thickness and mantle viscosity on glacially induced relative sea levels and long wavelength gravity field in a spherical, self-gravitating Maxwell Earth. Earth Planet Sci. Lett. 249 (3), 368–383.
Wells, D.L., Coppersmith, K.J., 1994. New Empirical relationships among magnitude, rupture length, rupture width, rupture area, and surface displacement. Bull. Seismol. Soc. Am. 84, 974–1002.
Williams, G.A., Turner, J.P., Holford, S.P., 2005. Inversion and exhumation of the St. George's Channel basin, offshore Wales, UK. J. Geol. Soc. 162, 97–110.
Wohlfarth, B., Luoto, T.P., Muschitiello, F., Väliranta, M., Björck, S., Davies, S.M., Kylander, M., Ljung, K., Reimer, P.J., Smittenberg, R.H., 2018. Climate and

environment in southwest Sweden 15.5-11.3 cal. Ka BP. Boreas. https://doi.org/10.1111/bor.12310.
Wu, P., 1997. Effect of viscosity structure of fault potential and stress orientations in eastern Canada. Geophys. J. Int. 130, 365–382.
Wu, P., 1998. Will earthquake activity in Eastern Canada increase in the next few thousand years? Can. J. Earth Sci. 35, 562–568.
Wu, P., 2004. Using commercial finite element packages for the study of earth deformations, sea levels and the state of stress. Geophys. J. Int. 158 (2), 401–408.
Wu, P., Hasegawa, H.S., 1996a. Induced stresses and fault potential in eastern Canada due to a disc load: a preliminary analysis. Geophys. J. Int. 125, 415–430.
Wu, P., Hasegawa, H.S., 1996b. Induced stresses and fault potential in Eastern Canada due to a realistic load: a preliminary analysis. Geophys. J. Int. 127, 215–229.
Wu, P., Johnston, P., 2000. Can deglaciation trigger earthquakes in N. America? Geophys. Res. Lett. 27, 1323–1326.
Wu, P., Wang, H., Steffen, H., 2013. The role of thermal effect on mantle seismic anomalies under Laurentia and Fennoscandia from observations of glacial isostatic adjustment. Geophys. J. Int. 192, 7–17.
Zhao, S., Lambeck, K., Lidberg, M., 2012. Lithosphere thickness and mantle viscosity inverted from GPS-derived deformation rates in Fennoscandia. Geophys. J. Int. 190 (1), 278–292.